

**R98-5.903.0009-4**

***Silicon-Based Nanostructural Ceramics Derived From  
Polymer Precursors: Development of Processing,  
Structure & Property Relationships***

**Final Technical Report**

**Prepared for:  
U.S. Air Force  
Air Force Office of Scientific Research  
Bolling AFB, DC 20332**

**Under Contract No. F49620-95-C-0020**

**Wayde R. Schmidt**

**October 15, 1998**

**"Approved for public release; distribution unlimited"**



**United  
Technologies**

**Research Center**

**Reproduced From  
Best Available Copy**

**DTIC QUALITY INSPECTED 3**

**19981202 007**

# REPORT DOCUMENTATION PAGE

AFRL-SR-BL-TR-98-

188

Public reporting burden for this collection of information is estimated to average 1 hour per response, including the time for reviewing the data needed, and completing and reviewing the collection of information. Send comments regarding this burden estimate or any other aspect of this collection of information, including suggestions for reducing this burden, to Washington Headquarters Services, Directorate for Information Operations and Reports, 1215 Jefferson Davis Highway, Suite 1204, Arlington, VA 22202-4302, and to the Office of Management and Budget, Paperwork Reduction Project (0704-0188).

hering  
ntorma-  
204.

0721

1. AGENCY USE ONLY (Leave blank)		2. REPORT DATE 15-Oct-98		3. REPORT TYPE AND DATES COVERED Final Technical Report 01 March 95 - 19 February 98	
4. TITLE AND SUBTITLE Silicon-Based Nanostructural Ceramics Derived From Polymer Precursors: Development of Processing, Structure & Property Relationships				5. FUNDING NUMBERS F49620-95-C-0020	
6. AUTHOR(S) Wayde R. Schmidt					
7. PERFORMING ORGANIZATION NAME(S) AND ADDRESS(ES) United Technologies Corporation United Technologies Research Center 411 Silver Lane East Hartford, CT 06108				8. PERFORMING ORGANIZATION REPORT NUMBER R98-5.903.0009-4	
9. SPONSORING/MONITORING AGENCY NAME(S) AND ADDRESS(ES) Dr. Alexander Pechenik Air Force Office of Scientific Research Directorate of Aerospace and Materials Sciences 110 Duncan Avenue Bolling AFB, D.C. 20332				10. SPONSORING/MONITORING AGENCY REPORT NUMBER	
11. SUPPLEMENTARY NOTES					
12a. DISTRIBUTION / AVAILABILITY STATEMENT Approved for public release; distribution unlimited.				12b. DISTRIBUTION CODE	
13. ABSTRACT (Maximum 200 words) This research program built on the knowledge gained under past AFOSR support and focused on developing additional basic understanding of the relationships between ceramic product and corresponding polymer precursor structures, as a function of processing conditions. The primary objectives for this work were to (1) demonstrate the use of silicon-based polymeric precursors as sources of nanostructured ceramic phases, including SiC, Si <sub>3</sub> N <sub>4</sub> , and SiC/AlN solid solutions; and (2) examine the ambient, as well as high temperature and high pressure behavior of these materials, including crystallization and polytype development, phase stability, densification and sintering characteristics.  Poly(methylvinylsilane) converts to C-rich, nanocrystalline $\beta$ -SiC during pyrolysis in argon, and the phase development is time and temperature dependent. Perhydropoly(silazane) provides a miscible source of elemental Si which effectively scavenges the excess C. Blends of the two polymers have increased ceramic char yields, and offer a source of SiC/Si <sub>3</sub> N <sub>4</sub> nanocomposites, especially near the stoichiometric ratio of excess Si to excess C. With blended polymers, crystal grain growth is inhibited below 1600 °C and sub-stoichiometric ratios, but is enhanced at higher temperatures due to phase separation and decomposition of the perhydropoly(silazane). Poly(aluminosilazanes) are effective single-source polymer precursors to SiC/AlN ceramic products. The molecular-level distribution of Si, C, Al, and N present in the room temperature reaction product is retained in the ceramic. The Si/Al ratio in the starting polymer determines the extent of crystallinity in the ceramic phase. Both 4- and 6-coordinate Al are observed, depending on the starting reactant ratio.					
14. SUBJECT TERMS preceramic polymers, nanocrystalline SiC, SiC/Si <sub>3</sub> N <sub>4</sub> nanocomposites, SiC/AlN solid solutions, poly(methylvinylsilane), poly(aluminosilazane)				15. NUMBER OF PAGES 66	
				16. PRICE CODE	
17. SECURITY CLASSIFICATION OF THIS REPORT Unclassified	18. SECURITY CLASSIFICATION OF THIS PAGE Unclassified	19. SECURITY CLASSIFICATION OF ABSTRACT Unclassified	20. LIMITATION OF ABSTRACT SAR		



**Research Center**

**R98-5.903.0009-4**

***Silicon-Based Nanostructural Ceramics Derived From Polymer  
Precursors: Development of Processing, Structure & Property  
Relationships***

**Final Technical Report**

**Contract F49620-95-C-0020**

Reported by: Wayde R. Schmidt  
Wayde R. Schmidt

Approved by: Foster P. Lamm  
Foster P. Lamm

**October 15, 1998**

## **TABLE OF CONTENTS**

	<b><u>Page</u></b>
<b>1.0 INTRODUCTION AND BACKGROUND.....</b>	<b>1</b>
<b>2.0 TECHNICAL DISCUSSION.....</b>	<b>2</b>
<b>2.1 Precursors to Silicon Carbide and Silicon Nitride .....</b>	<b>2</b>
2.1.1 Synthesis .....	2
2.1.2 Polymer-to-Ceramic Conversion .....	3
2.1.3 Phase Development .....	4
2.1.4 Densification of Nanocrystalline SiC Powders.....	6
<b>2.2 Precursors to Silicon Carbide/Aluminum Nitride Solid Solutions .....</b>	<b>8</b>
2.2.1 Synthesis .....	8
2.2.2 Polymer-to-Ceramic Conversion .....	9
2.2.3 Phase Development .....	9
<b>3.0 SUMMARY/CONCLUSIONS.....</b>	<b>11</b>
<b>4.0 REFERENCES.....</b>	<b>12</b>
<b>5.0 ACKNOWLEDGMENTS.....</b>	<b>14</b>
<b>6.0 PERSONNEL SUPPORTED .....</b>	<b>14</b>
<b>7.0 PUBLICATIONS AND PRESENTATIONS .....</b>	<b>15</b>

**FIGURES 1-49**



## **SILICON-BASED NANOSTRUCTURAL CERAMICS DERIVED FROM POLYMER PRECURSORS: DEVELOPMENT OF PROCESSING, STRUCTURE AND PROPERTY RELATIONSHIPS**

### **1.0 INTRODUCTION AND BACKGROUND**

Non-oxide engineering ceramics such as SiC and Si<sub>3</sub>N<sub>4</sub> are promising structural materials for Air Force applications requiring high temperature stability, load-bearing capability, low density, chemical resistivity, good strength, toughness, thermal shock resistance and hardness. These materials and their composites are finding applications in forming wear- and corrosion-resistant components of combustion/heat engines, furnaces, valves, turbines and supersonic vehicles. The development of economical processing methods for fabricating these ceramics into fully dense, non-brittle near-net shapes, which require minimal final machining, is critical for both the wide-spread implementation of such materials and the full realization of the intrinsic properties of these ceramics.

For monolithic bodies, current ceramic processing methods such as slip casting, dry pressing, freeze casting, isostatic pressing and injection molding require careful control of the particle size and particle size distribution of the starting ceramic powders. Densification generally involves a multiple step process that includes the addition of organic binders or low melting, oxide glass-forming sintering aids, high temperatures, externally applied high pressure, or some combination of these methods. In each case, residual impurities and excessive temperatures can reduce the properties of the resulting ceramic component relative to the base ceramic.

Chemical processing methods have proven effective as routes to prepare homogeneous, high purity single- and multi-phase nanosized ceramic powders for structural applications. Past studies have focused on the deformation of nanocrystalline materials or superplasticity of materials derived from sol-gel techniques<sup>1,2</sup>, solution precipitation<sup>2</sup>, or gas condensation of finely divided metal, followed by oxidation<sup>3</sup> to prepare oxide powders; and vapor phase condensation followed by thermal decomposition of organometallic precursors<sup>4</sup> or reactions between volatile silicon-containing species and NH<sub>3</sub>/N<sub>2</sub> to prepare mixed SiC/Si<sub>3</sub>N<sub>4</sub> non-oxide phases<sup>5,6</sup>. In the latter cases, oxide sintering aids were generally added to improve densification of the powders prior to mechanical testing. Only recently have researchers considered organometallic polymers as useful sources of nanocrystalline ceramics<sup>7,8</sup>.

Organometallic polymeric precursors to ceramic phases are also receiving attention for fabricating components in high temperature structural applications. Much of the interest in these systems lies in the potential, through chemical manipulation at near ambient conditions, to (1) control the resulting phase composition and homogeneity; (2) prepare fine-grained materials at relatively low processing temperatures; and (3) generate useful forms of the ceramics, including continuous fiber, film, powders, or composite matrix phases. Examples

of such polymer-derived ceramic products include Dow Corning's Sylramic™ SiC fiber, Nippon Carbon's Nicalon™ SiCO fiber, Allied Signal's Blackglas™ poly(siloxane) resins for SiOC phases, University of Florida's stoichiometric SiC fiber, and Bayer Corporation's developmental poly(borosilazane)-derived SiBNC products.

A previous AFOSR-sponsored research program at the United Technologies Research Center (UTRC) focused on the development of a family of novel Si-containing organometallic polymers (poly(methylvinylsilanes)) and polymer blends<sup>9</sup>. These systems were useful as precursors to nanometer-sized crystals of SiC and homogeneous alloys of nanocrystalline SiC and Si<sub>3</sub>N<sub>4</sub><sup>9</sup>. UTRC used these polymers in this research program to prepare Si-based nonoxide ceramics with controlled phase composition, morphology and purity, and new ceramic blends containing atomically distributed phases with specific structures. In this manner, chemical processing, and specifically, the pyrolytic conversion of preceramic polymers, was used to engineer ceramic nanocomposite structures.

The research program summarized in this report built on the knowledge gained under past AFOSR support and attempted to develop additional basic understanding of the relationships between ceramic product and corresponding polymer precursor structures, as a function of processing conditions. The primary objectives for this work were to (1) demonstrate the use of silicon-based polymeric precursors as sources of nanostructured ceramic phases, including SiC, Si<sub>3</sub>N<sub>4</sub>, and SiC/AlN solid solutions; and (2) examine the ambient, as well as high temperature and high pressure behavior of these materials, including crystallization and polytype development, phase stability, densification and sintering characteristics.

## 2.0 TECHNICAL DISCUSSION

### 2.1 Precursors to Silicon Carbide and Silicon Nitride

#### 2.1.1 Synthesis

Prior work at UTRC under partial AFOSR sponsorship resulted in the synthesis of a novel series of polysilane precursors and blends to ceramics containing SiC<sup>9</sup>. Poly(methylvinylsilane), (PMVS; average structure:  $[(CH_2=CH)Si(CH_3)]_n$ ), was synthesized as the precursor to C-rich  $\beta$ -SiC. Perhydropoly(silazane), (PHPS; average structure:  $[H_2SiNH]_n$ ), was purchased from Tonen as the precursor to Si-rich  $\alpha$ -Si<sub>3</sub>N<sub>4</sub> and was used to prepare mechanical blends with PMVS (Table 1). The synthesis schemes for these polymers are shown in Figures 1 and 2, respectively.

FAR Research, Inc., Palm Bay, FL, a manufacturing company specializing in the synthesis of silicon-based compounds, expressed interest in preparing the PMVS precursor on a pilot plant scale. Under subcontract to UTRC, FAR successfully demonstrated the scalability of the PMVS synthesis by producing nearly 1 kg of polymer in a single batch

process. Even larger scale synthesis of the PMVS-based materials would significantly reduce the product cost while also improving product consistency and quality.

**TABLE 1**  
**BLEND COMPOSITIONS OF PMVS/PHPS BASED ON CHAR**  
**ANALYSIS AFTER PYROLYSIS OF PMVS TO 1000 °C IN ARGON<sup>9</sup>.**

Blend Code	Weight % PMVS	Moles excess Si from PHPS per mole of excess C from PMVS
A (PMVS only)	100.0	0
B	50.0	0.25
C	33.3	0.50
D	20.0	1.0
E	14.4	1.5
F	11.2	2.0
G	2.5	10.0
H (PHPS only)	0	∞

### 2.1.2 Polymer-to-Ceramic Conversion

Thermal analysis of PMVS/PHPS blends in argon showed enhanced ceramic char yields at 1000 °C (Figure 3; for 2 °C/min heating rates, up to 82% of the original sample weight was retained, depending on the PMVS/PHPS ratio) when compared to either pure PMVS (43%) or PHPS (57%). Higher yields are desirable to minimize shrinkage that is typically associated with preceramic polymers, and to reduce costs associated with wasted materials or the extra processing steps required to increase part density. Characterization of the converted polymer blends by infrared spectroscopy indicated that below 200 °C, a beneficial hydrosilylation reaction occurred between the vinyl groups ( $-\text{CH}=\text{CH}_2$ ) of the PMVS and the silyl groups ( $\equiv\text{Si-H}$ ) of the PHPS. Such a reaction increases the crosslinking density of the polymer network, thereby increasing the molecular weight of the polymer, and results in an increased ceramic char yield.

By varying the ratio of PMVS to PHPS in the blend, the relative ratio of  $\text{SiC}$  to  $\text{Si}_3\text{N}_4$  in the ceramic product, obtained following pyrolysis in argon, was controlled. Stock blends of PMVS/PHPS were pyrolyzed in argon to 1000 °C and subsequently heated to temperatures as high as 2000 °C in flowing argon or nitrogen for 1 hour to examine the effect of temperature on sample crystallinity. Select blend compositions were heated from 1200 °C to 1800 °C in argon for 1, 2, 4 or 8 hours. Characterization of these samples included analysis by powder X-ray diffraction (XRD), transmission electron microscopy (TEM), and solid-state nuclear magnetic resonance spectroscopy (SSNMR).

### 2.1.3 Phase Development

XRD techniques provided insight into the composition of crystalline phases and, through peak broadening measurements, information on crystal size. Results obtained during Year 1 of this AFOSR program showed that PMVS converts to C-rich nanocrystalline  $\beta$ -SiC upon pyrolysis to 1000 °C in either argon or nitrogen. A series of experiments was performed in which powder samples of PMVS were heated in argon at temperatures up to 1800 °C for 1 to 8 hours, followed by XRD analysis to examine sample crystallization kinetics (Figures 4 and 5). Results shown in Figure 5 indicate that the crystallization of  $\beta$ -SiC from PMVS was both time and temperature dependent. Crystallization was fairly sluggish for all treatment times from 1000-1400 °C, but increased significantly above 1400 °C. For example, below 1400 °C, the  $\beta$ -SiC crystal size (extracted from powder diffraction peak width data) was 5 nanometers or less at all heating times. In contrast, by 1800 °C, crystal size increased to 20-30 nanometers, and was generally larger with longer heat times and higher temperatures. Following heating to 2000 °C, crystals had grown to greater than 100 nanometers. XRD also indicated that heating to 1800-2000 °C caused the excess C that was originally present in the PMVS polymer to crystallize to graphite. Complementary TEM analysis showed a homogeneous distribution of equiaxed, nanosized  $\beta$ -SiC crystals at each temperature, and showed that below 1000 °C, the crystals were typically less than 1 nanometer in diameter.

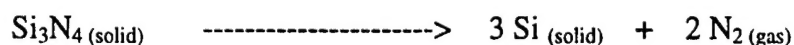
Perhydropoly(silazane), PHPS, was determined previously under AFOSR sponsorship to provide Si-rich  $\text{Si}_3\text{N}_4$  upon pyrolysis in argon<sup>9</sup>. Polymer blends of PMVS and PHPS were prepared in attempts to (1) provide a molecularly-distributed source of excess Si to scavenge the excess C from PMVS; (2) examine the effect of composition on the crystallization behavior of the resulting ceramics; and (3) identify suitable precursors to homogeneous SiC/ $\text{Si}_3\text{N}_4$  composite powders.

Various blends of PMVS and PHPS (Table 1) were prepared and pyrolyzed in argon to temperatures up to 1800 °C for 1 to 8 hours. Samples of PMVS and PMVS/PHPS blends that were pyrolyzed in argon below 1000 °C can be considered "amorphous", although they actually consist of nanocrystalline SiC. With additional heating at elevated temperatures, broad peaks develop for the planes of  $\beta$ -SiC, which sharpen with increased temperature and time.

XRD analysis of the ceramic chars from the blends showed significant effects of the starting blend composition on the phase distribution and the extent of crystallinity in the ceramic powders. In general, ceramic chars of PMVS/PHPS blends from pyrolysis in argon show reduced crystallinity and/or inhibition of grain growth below 1600 °C (relative to PMVS only) and stabilization of the nanostructure due to the molecular-level mixing of the components. Above 1600 °C, however, the blends show enhanced SiC grain growth due to  $\text{Si}_3\text{N}_4$  decomposition (and resulting phase separation) into highly reactive nuclei of elemental Si and volatile  $\text{N}_2$ . For example, a blend composition containing a relatively low molar amount of excess Si from PHPS, e.g. Si/C=0.25 (Figure 6), showed broader and less intense XRD peaks at 1400 °C and below, indicating a reduced level of crystallinity relative to the pure PMVS (Figure 4). However, at 1600 °C and above, the XRD peaks were much sharper,

which indicated that the crystallinity of the  $\beta$ -SiC was greatly enhanced. For this composition, no phases other than  $\beta$ -SiC were observed by XRD.

When the level of excess Si was increased, as in the blend composition with Si/C=0.5 (Figure 7), peaks indicating  $\beta$ -SiC and new peaks corresponding to  $\alpha$ -Si<sub>3</sub>N<sub>4</sub> were observed in the diffraction pattern of the sample heated to 1600 °C. At 1400 °C and below, the broad peaks of the XRD pattern indicated reduced crystallinity in the  $\beta$ -SiC phase and the absence of any Si<sub>3</sub>N<sub>4</sub> phase. The sample heated to 1800 °C provided an X-ray diffraction pattern that was intriguing. In this case; the  $\beta$ -SiC crystallinity was greatly enhanced, but no pattern indicative of Si<sub>3</sub>N<sub>4</sub> was present. Instead, sharp peaks were observed which indicated the presence of elemental Si; this is consistent with a decomposition mechanism of the polymer-derived Si<sub>3</sub>N<sub>4</sub> in an argon atmosphere into elemental Si and gaseous N<sub>2</sub>.



Apparently, the presence of elemental Si in the ceramic blend enhanced the crystallinity of the SiC. A control experiment was performed to test this hypothesis, in which the identical blend sample was heated to 1600 °C in N<sub>2</sub> in an attempt to stabilize the Si<sub>3</sub>N<sub>4</sub> phase. XRD analysis of the ceramic product showed the presence of crystalline  $\alpha$ -Si<sub>3</sub>N<sub>4</sub>, no elemental Si, and  $\beta$ -SiC that was greatly reduced in crystallinity (Figure 8).

X-ray diffraction also showed the dependence of crystallinity and phase development on time for several of the PMVS/PHPS blend samples. Figure 9 shows the result of one experiment in which the blend composition corresponding to Si/C=0.5 was heated at 1400 °C in argon for 1, 2, 4, or 8 hours. XRD showed the sample to be nanocrystalline  $\beta$ -SiC after 1 or 2 hours of heating. After 4 or 8 hours, the diffraction peaks of the  $\beta$ -SiC had sharpened due to grain growth, but new peaks corresponding to nanocrystalline  $\alpha$ -Si<sub>3</sub>N<sub>4</sub> were also present. This data confirmed the presence of both SiC and Si<sub>3</sub>N<sub>4</sub> in the sample.

Corresponding TEM analysis using small area electron diffraction (SAED) confirmed the nanocrystalline nature of the ceramic phases (Figures 10-16) and provided additional evidence for SiC/Si<sub>3</sub>N<sub>4</sub> nanocomposite formation, especially near the stoichiometric ratio of excess Si/excess C in the polymer blends heated to relatively low temperature (Figure 15). SiC whiskers were observed in some of the pyrolyzed blended samples (Figures 11 and 12), perhaps formed by a dissolution/re-precipitation mechanism of the SiC in elemental Si near its melting point (1410 °C).

Solid-state <sup>29</sup>Si NMR was used to probe the chemical bonding environments of the Si nuclei in the ceramic products. Figure 17 shows a series of SSNMR spectra of blend samples that were heated briefly to 1600 °C in argon. The series showed that the SiC and Si<sub>3</sub>N<sub>4</sub> phases were chemically distinct – i.e. two separate peaks corresponding to SiC<sub>4</sub> and SiN<sub>4</sub> bonding environments were identified. The peak separation is most noticeable beginning at stoichiometric ratios, and it is expected that the level of phase separation is both time and temperature dependent. These data also relates to the decomposition of the PHPS-derived Si<sub>3</sub>N<sub>4</sub> in argon at higher temperatures (Figure 9).



## 2.1.4 Densification of Nanocrystalline SiC Powders

Results obtained during Year 2 of this AFOSR program focused on preliminary sintering experiments to determine the densification behavior of the polymer-derived ceramics using conventional sintering aids. Experiments were performed by ball milling mixtures of ceramic char, 4 wt%  $\text{Al}_2\text{O}_3$ , 4 wt%  $\text{Y}_2\text{O}_3$  and 8 wt% of PMVS polymer as a binder in "dry" hexane (Figure 18). The ceramic chars were prepared by the thermal decomposition of several blend compositions of PMVS and PHPS. Following removal of the solvent and drying, pellets were uniaxially pressed to 60 ksi for 1 minute and subsequently fired in argon to 1000 °C for 1 hour prior to sintering experiments.

Pellets were fired for 2 hours at temperatures ranging from 1000-1900 °C using one of the following conditions: (a) argon atmosphere plus SiC powder bed; (b)  $\text{N}_2$  atmosphere plus SiC powder bed; or (c)  $\text{N}_2$  atmosphere plus  $\text{Si}_3\text{N}_4$  powder bed. The results of these experiments are presented in Figures 19-25, including comparative density data obtained in experiments using Aerochem's developmental nanocrystalline  $\beta$ -SiC and Washington Mills commercial grade  $\alpha$ -SiC. Pellets made from PMVS only (Figure 21) showed increased density above 1600 °C under condition (a), while density decreased slightly above that temperature under condition (b). The use of the  $\text{Si}_3\text{N}_4$  bed in (c) offered no major improvement at 1800 °C. For polymer blends containing an increased amount of PHPS-derived  $\text{Si}_3\text{N}_4$  (Figures 22 and 23), pellet densities increased significantly between 1400 °C and 1600 °C, but decomposition through  $\text{N}_2$  loss resulted in severely decreased density above 1600 °C. Pellet decomposition was retarded significantly with the use of a  $\text{N}_2$  atmosphere with condition (b), and was further retarded with the use of a  $\text{Si}_3\text{N}_4$  powder bed as in (c).

In collaboration with Prof. Bogdan Palosz of the High Pressure Research Center (UNIPRESS) in Warsaw, Poland, additional polymer-derived char samples of SiC and SiC/ $\text{Si}_3\text{N}_4$  (previously pyrolyzed to temperatures up to 1800 °C) were subjected to high applied pressures at temperatures as high as 1700 °C (without the addition of sintering aids) using a cubic WC or diamond anvil cell. Microstructural analysis, predominantly TEM, was performed on these densified samples. In addition to UTRC, Prof. Palosz also collaborated with Dr. David Keil at Aerochem, to evaluate high pressure densification of Aerochem's nanocrystalline SiC. An experimental program was also established with Dr. Stephen Danforth at Rutgers University to evaluate the sintering behavior of highly pure, nanocrystalline SiC in the presence of high purity nanocrystalline  $\text{Al}_2\text{O}_3$  and  $\text{Y}_2\text{O}_3$  sintering aids. Unfortunately, program funding was unavailable to continue these collaborative research efforts.

Interactions with Prof. Palosz established that there is significant evidence that SiC alone does not sinter, possibly because the ratio of grain boundary to surface energy,  $\gamma_{\text{gb}}/\gamma_{\text{sv}}$ , is too high for SiC and that there is a thermodynamic limit with respect to the sinterability of SiC. Because of this, pure  $\beta$ -SiC in sintered form is generally not available as a structural ceramic material. Pressureless sintering of SiC requires temperatures approaching 2200 °C and regardless of starting material, results in hexagonal  $\alpha$ -SiC. Cubic  $\beta$ -SiC, however, is expected to have superior properties over  $\alpha$ -SiC, based on symmetry considerations and

because of its ductility at elevated temperatures<sup>10</sup>. Because high pressure is known to promote the formation of  $\beta$ -SiC<sup>11-15</sup>, another study examined the use of high pressure to form dense ceramic bodies, at relatively low temperatures and without the intentional addition of sintering aids. The unique physical properties of nanocrystalline  $\beta$ -SiC, as prepared by preceramic polymers, were expected to enhance the potential for obtaining dense  $\beta$ -SiC ceramic.

*In-situ* diffraction experiments on sintering were performed with the use of the cubic anvil cell MAX80 at HASYLAB working in the energy dispersive geometry (Figure 26). The maximum applied pressure was 7.0 GPa at temperatures up to 1700 °C (controlled to an accuracy of 50 °C). Samples were pressurized up to 4 GPa and then heated in steps of 100-200 °C to the desired temperature. After 30-40 minutes of annealing at temperature, the samples were cooled to room temperature and the pressure was released to 1 atmosphere.

Due to the strong asymmetric broadening of the Bragg lines under pressure, the *in-situ* diffraction data were not used for structural analysis of disordering; this analysis was instead based on the intensity profiles measured at room temperature after the release of pressure. Samples were pressurized both (i) hydrostatically at room temperature, using petroleum jelly as a pressure-transfer medium, and (ii) isostatically, without pressure medium; these samples were sintered at high temperatures.

Structural analysis was based on the modeling of disordered structures and computer simulation of powder diffraction profiles<sup>16</sup> (Figures 27-29). Experimentally measured Bragg reflections were modeled with the use of a PeakFit program, using a combination of two symmetrical functions, Gaussian (G) and Lorentzian (L), which were each described by a position and half-width. In unstrained material, these peak shape components occur at the same position, but under pressure and elevated temperatures, they behave very differently. The extracted parameters describing the G and L functions were used to examine sample compressibilities and microstrain. Based on the structural model of disordered SiC (Figure 27), there was a good comparison between the calculated and the experimental diffraction patterns for cubic-like domains on the order of 10 nm and 70-85 nm (Figure 29).

Under *hydrostatic* pressure using the MAX80 cubic anvil cell, there was practically no peak broadening effect on the nanocrystalline SiC up to 6 GPa; an indication that no microstrain was induced during the experiment, and confirmation that the experiment was indeed hydrostatic (Figure 30). These results also held true for microcrystalline SiC. *Isostatic* conditions, however, induced inhomogeneous strain into the polycrystals. The Bragg peak of the strained material dissociated into two components, G and L, which may suggest separate fractions of the SiC (presumably with the same chemical composition) with different compressibilities of their respective lattices (Figure 31). Annealing of the isostatically strained materials under pressure leads to relaxation of the microstrain, as indicated by both a decrease in the broadening of the Bragg lines, as well as a reduction in the difference between interlayer spacings of the G- and L-related fractions (Figure 32).

Preliminary results from compressibility studies using the Diamond Anvil Cell provided additional insight into the behavior of polymer-derived nanocrystalline SiC. PMVS,

previously annealed to 1600 °C in argon, undergoes two changes in the slope of the lattice parameter vs. pressure plot, and appears to become "softer" (more compressible) with increased pressure (Figure 33). PMVS and PMVS/PHPS-C heated to 1800 °C (Figures 33 and 34), however, become significantly "harder" (less compressible) under similar experimental conditions. The compressibility plot for microcrystalline  $\beta$ -SiC (prepared by SHS) shows a single slope change in Figure 34. The cause of the observed "kink" in the plots of PMVS (1600 °C) and PMVS/PHPS-C (1800 °C) is unknown at this time.

In conjunction with Rutgers University, work was initiated to examine the pressureless sintering behavior of highly pure nanocrystalline SiC in the presence of nanocrystalline sintering aids. Unfortunately, the program was stopped before any significant results could be achieved.

## 2.2 Precursors to Silicon Carbide/Aluminum Nitride Solid Solutions

Conventional methods to form solid solutions suffer from unacceptable levels of impurities and the inability to easily shape the final ceramic into workable parts<sup>17</sup>. The use of polymer precursors provides the potential for more control of composition, decreased impurity levels, and the ability to shape or mold the final ceramic, as well as to reduce manufacturing costs<sup>18</sup>. SiC/AlN solid solutions have been prepared by the copolyolysis of two separate precursors. Czekaj et al.<sup>19</sup> pyrolyzed dialkyl aluminum amide compounds with either polycarbosilane or vinylic polysilane. Schmidt et al.<sup>20</sup> prepared SiC/AlN from a single-source precursor made by the reaction of alkylaluminum compounds and 1,3,5-trimethyl-1,3,5-trivinylcyclotrisilazane. Paine and co-workers have investigated the preparation of  $[(\text{Me}_3\text{Si})_2\text{AlNH}_2]_2$  and its pyrolysis to form SiC/AlN mixtures<sup>21,22</sup>.

### 2.2.1 Synthesis

All chemicals and isolated products were handled in either a  $\text{N}_2$ -filled glovebox ( $\text{H}_2\text{O}$ ,  $\text{O}_2 < 2$  ppm) or using Schlenk techniques due to the pyrophoric nature of alkylaluminum compounds and the moisture sensitivity of high surface area ceramic powders. A series of single-source poly(aluminosilazane) precursors (PAS) to SiC/AlN was prepared by reacting hexamethylcyclotrisilazane (HMTS),  $[(\text{CH}_3)_2\text{SiNH}]_3$ , with triethylaluminum (TEA),  $[(\text{CH}_3\text{CH}_2)_3\text{Al}]$ , either neat or with both components dissolved in dry hexane at room temperature, as schematically represented in Figure 35. One mole of HMTS contains 3 moles of Si and 3 moles of N, while there is only 1 mole of Al per mole of TEA. Thus, to achieve an equimolar ratio of Si and Al in the PAS polymer, 1 mole of HMTS per 3 moles of TEA are required. Polymer compositions were designed by varying the ratio of HMTS to TEA in the reaction, so that the Si/Al ratio in the initial reaction, as well as the resulting polymer, ranged from 1 to 10. Polymerization occurred with the exothermic evolution of ethane gas.

Polymerization was monitored by infrared spectroscopy and the N-H functionality near  $3400\text{ cm}^{-1}$  was seen to decrease with time, as well as with increased Al content, as the N-Al linkages were formed (Figures 36 and 37). This technique confirmed the presence of



unreacted N-H functionality for reactions with Si/Al above 5, and showed the complete consumption of the N-H structure for a Si/Al ratio near 1. The surprising discovery was that new N-H bonding structure develops in polymers with Si/Al ratios between 1.5 and 3. This new functionality apparently promotes polymer crosslinking, and subsequent increases in molecular weights. Network polymer formation was dependent on the ratios of the starting reactants; e.g. polymers were noticeably less viscous as the Si/Al ratio increased, probably because of the increasing amount of unreacted N-H groups from the HMTS. Isolated polymers ranged in consistency from thin oily liquids (Si/Al above 5), to sticky, taffy-like pastes (Si/Al near 1), to brittle solids (Si/Al from 1.5 to 2). As expected, polymers with relatively low Si/Al ratios, especially those with Si/Al less than 1.5, were more pyrophoric.

The high viscosity and sticky nature of several of the polymers suggests that they would be useful to draw fibers. In fact, fiber strands could be manually pulled from these samples. Controlled production of ceramic fibers, however, requires curing the polymer prior to pyrolytic conversion. Several samples of PAS polymers were supplied to Professor Michael Sacks at the University of Florida, Gainesville, for incorporation into his stoichiometric SiC fiber formulations.

### 2.2.2 Polymer-to-Ceramic Conversion

Thermal analysis was used as a convenient method to examine sample weight loss as a function of temperature. The ceramic yield of the PAS polymers tended to decrease with increasing fluidity, ranging from approximately 60% for polymers with Si/Al ratios from 1 to 3, to below 30% for those prepared using Si/Al ratios above 5 (heating ramp of 10 °C/min in flowing N<sub>2</sub>). A representative TGA plot is shown in Figure 38 for PAS with Si/Al equal to 3.

In separate studies, three series of PAS samples were prepared. The first series used the PAS polymer with a Si/Al ratio equal to 1. Samples of this polymer were pyrolyzed in N<sub>2</sub> from 200 °C to 1800 °C, held at temperature for 1 hour, and cooled to room temperature. The second series used the PAS polymer with Si/Al equal to 3 for similar heat treatments. The third series varied the starting Si/Al ratio from 1 to 5 and varied the heat treatment temperature as high as 1800 °C. Processed samples from each of the series of experiments were subsequently analyzed by X-ray diffraction, transmission electron microscopy, and solid state NMR techniques.

### 2.2.3 Phase Development

XRD powder patterns of samples with a Si/Al ratio equal to 1 showed increased crystallinity with increased temperature, especially at 1200 °C and higher (Figure 39), where the pattern indicating the solid solution was evident. Transmission electron microscopic examination showed the crystals were typically plate-like and highly faulted, with regions of relatively high concentrations of Al (Figures 40-42). <sup>27</sup>Al NMR showed a single peak which shifted from 103 ppm to 110 ppm with increased temperature from 1000 °C to 1600 °C. This peak confirmed the presence of AlN<sub>4</sub> bonding environments as would be expected in AlN (Figure 43). Samples in which the Si/Al ratio was 3 showed similar results. However, the

XRD series and TEM results showed generally reduced crystallinity and grain size (Figures 44-46), and the sharp peaks of the solid solution pattern do not appear until 1800 °C (Figure 44).

The program results demonstrated that the amount of Al present in the starting polymer significantly affected the extent of crystallinity in the ceramic product. For example, XRD analysis indicated that as the molar ratio of Si/Al increased from 1 to 5, the overall crystallinity of the solid solution decreased (Figure 47). Regardless of the Si/Al ratio in the starting polymer, phase pure 2H wurtzite-type structure (SiC/AlN solid solution) was produced with heat treatment (Figures 39, 44, 47). This result is consistent with the observations that the presence of Al or AlN stabilizes the hexagonal ( $\alpha$ ) polytype of SiC. The unique aspect of this contract work is that single-source polymers were used to produce this stabilized ceramic structure.

A detailed examination of the (110) plane in the XRD patterns indicated that the peak position shifted with the ratio of Si/Al in the starting PAS polymer (Figure 48). As expected, as the amount of Si in the starting polymer increased, the crystal phase was more likely to be richer in SiC, and the position of the (110) peak was nearer to that expected for pure SiC. Likewise, samples containing more Al had the (110) peak nearer to that of pure AlN.

TEM coupled with energy dispersive X-ray spectroscopy (EDS) also confirmed that the relative molar ratios of Si and Al in the starting polymers were retained in the ceramic products. There was evidence in several samples that some phase separation of the material into Al- and Si-rich regions had occurred. This result has been observed by other researchers using solid solutions prepared by traditional ceramic powder methods combined with hot pressing, and is consistent with the phase diagram proposed for the SiC/AlN system by Zangvil and Ruh<sup>23</sup>. Those researchers indicate that a phase separation of the single phase 2H solid solution ( $\delta$ ) occurs below 2000 °C into  $\delta_1$  and  $\delta_2$  phases.

<sup>27</sup>Al and <sup>29</sup>Si magic angle spinning (MAS) solid-state nuclear magnetic resonance (NMR) spectroscopy was used to analyze the PAS samples in terms of coordination number, nearest neighbor atoms, and crystallinity. Purity, as defined by the presence of SiC<sub>4</sub> and AlN<sub>4</sub> units (expected in pure SiC and AlN), and crystallinity increased with increasing temperature and decreased with increasing Si(N)/Al ratio. For relatively low concentrations of Al, as in PAS with Si/Al equal to 1.0, solid-state <sup>27</sup>Al NMR showed bonding typical of AlN<sub>4</sub> environments as anticipated for AlN (Figure 49). The spectral peaks sharpened in samples heated to higher temperatures, which is consistent with increased crystallinity and ordering in the samples (and consistent with XRD results). The exciting results were observed for samples with decreased Al concentrations (Figure 49). In addition to AlN<sub>4</sub> bonding environments, the PAS polymer with Si/Al of 5.0 showed <sup>27</sup>Al NMR spectral peaks that were consistent with Al nuclei that are coordinated to 6 N atoms, as in AlN<sub>6</sub>.

### 3.0 SUMMARY/CONCLUSIONS

- PMVS converts to C-rich, nanocrystalline  $\beta$ -SiC during pyrolysis in argon, and the phase development is time and temperature dependent.
- PHPS provides a miscible, homogeneous source of elemental Si, which can effectively scavenge the excess C from PMVS.
- Blends of PMVS and PHPS have higher char yields (70-85%) than either polymer alone.
- Preceramic polymer blends provide evidence for nanocomposite formation ( $\beta$ -SiC and  $\alpha$ -Si<sub>3</sub>N<sub>4</sub>), especially near the stoichiometric ratio of excess Si/excess C.
- Grain growth is inhibited in blended PMVS/PHPS at relatively low temperatures (<1600 °C) and sub-stoichiometric ratios, but is enhanced at higher temperatures due to phase separation.
- PHPS-derived Si<sub>3</sub>N<sub>4</sub> decomposes to elemental Si and N<sub>2</sub> in argon; Si<sub>3</sub>N<sub>4</sub> is stabilized in N<sub>2</sub>, but SiC crystallinity decreases.
- Simulation of X-ray diffraction patterns, combined with a one-dimensional disorder model, indicates a high degree of disorder for polymer-derived, nanocrystalline SiC.
- The nano-sized grains of polymer-derived SiC severely restrict the formation of additional dislocations, as well as the conversion of  $\beta$ -SiC to the  $\alpha$ -SiC polytype. Transformation occurs through recrystallization into pure 3C structure rather than via generation of stacking disorders.
- Changes in the lattice parameters (compressibility) and peak widths (microstrain) at high pressures are strongly dependent on the grain size of the nanocrystalline SiC, and suggest the excellent potential for sintering nano-SiC to full density 3C at relatively low temperatures.
- Poly(aluminosilazanes) are effective polymer precursors to SiC/AlN ceramic products. The molecular-level distribution of Si, C, Al, and N are present in the room temperature reaction product and is retained in the ceramic product.
- Increased temperature causes increased grain growth of PAS-derived chars to single phase wurtzite (XRD powder pattern indicates single phase solid solution).
- The Si/Al ratio in the starting polymer determines the extent of crystallinity in the ceramic phase. As the Si/Al ratio increases from 1 to 5, the extent of crystallinity

generally decreases. The (110) XRD peak shifts to higher  $2\theta$  with increasing Si/Al ratio.

- $^{27}\text{Al}$  SSNMR confirms the presence of 4-coordinate Al in all polymers heated to 1200 °C in  $\text{N}_2$ . However, as the Si/Al ratio increases above 3, 6-coordinate Al is also observed as  $\text{AlN}_6$ .
- TEM/EDS analysis suggest an inhomogeneous distribution of Al and/or Si in PAS-derived ceramics. This evidence supports some phase separation of the SiC/ $\text{AlN}$   $2H$  solid solution below 2000 °C.

#### 4.0 REFERENCES

1. I.-W. Chen and L. A. Xue, "Development of Superplastic Structural Ceramics", *J. Am. Ceram. Soc.*, **73**[9] (1990) 2585-2609.
2. M. J. Mayo, D. C. Hague and D.-J. Chen, "Processing Nanocrystalline Ceramics for Applications in Superplasticity", *Mater. Sci. and Eng.*, **A166**[1-2] (1993) 145-159.
3. J. Karch, R. Birringer and H. Gleiter, "Ceramics Ductile at Low Temperature", *Nature*, **330**[10 Dec 1987] 556-558.
4. W. Chang, G. Skandan, H. Hahn, S. C. Danforth and B. H. Kear, "Chemical Vapor Condensation of Nanostructured Ceramic Powders", *NanoStructured Materials*, **4**[3] (1994) 345-51.
5. a) F. Wakai, Y. Kodama, S. Sakaguchi, N. Murayama, K. Izaki and K. Niihara, "A Superplastic Covalent Crystal Composite", *Nature*, **344**[29 Mar 1990] 421-423; b) F. Wakai, Y. Kodama, S. Sakaguchi, N. Murayama, K. Izaki and K. Niihara, "Superplasticity of Non-Oxide Ceramics", *Mat. Res. Soc. Symp. Proc.*, **196** (1990) 349-358; c) F. Wakai, S. Sakaguchi and Y. Matsuno, "Superplasticity of Yttria-Stabilized Tetragonal  $\text{ZrO}_2$  Polycrystals", *Adv. Ceram. Mater.*, **1**[3] (1986) 259.
6. T. Rouxel, F. Wakai and K. Izaki, "Tensile Ductility of Superplastic  $\text{Al}_2\text{O}_3$ - $\text{Y}_2\text{O}_3$ - $\text{Si}_3\text{N}_4$ /SiC Composites", *J. Am. Ceram. Soc.*, **75**[9] (1992) 2363-2372.
7. a) L. V. Interrante, W. J. Hurley, Jr., W. R. Schmidt, D. Kwon, R. H. Doremus, P. S. Marchetti and G. E. Maciel, "Preparation of Nanocrystalline Composites by Pyrolysis of Organometallic Precursors", *Ceramic Transactions Vol. 19 Advanced Composite Materials*, American Ceramic Society, Westerville, OH, pp. 3-17, (1991); b) L. V. Interrante, W. R. Schmidt, P. S. Marchetti and G. E. Maciel, "Pyrolysis of Organometallic Precursors as a Route to Novel Ceramic Materials", *Mat. Res. Soc. Symp. Proc.*, **249** (1992) 31-43.

8. a) M. Nowakowski, K. Su, L. Sneddon and D. Bonnell, "Synthesis, Processing and Phase Evolution of TiN/TiB<sub>2</sub> Composites from Polymeric Precursors", *Mat. Res. Soc. Symp. Proc.*, **286** (1993) 425; b) Z. Jiang and W. E. Rhine, "Preparation of Nanophase SiC/Si<sub>3</sub>N<sub>4</sub>, SiC/B<sub>4</sub>C and Stoichiometric SiC from Mixtures of a Vinylic Polysilane and Metal Powders", *Mat. Res. Soc. Symp. Proc.*, **286** (1993) 437.
9. W. R. Schmidt, "Novel Precursor Approaches for CMC Derived by Polymer Pyrolysis", Final Technical Report for AFOSR Contract F49620-91-C-0017, UTRC Report R94-970051-3, 15 February 1994.
10. S. Tsurekawa, Y. Hasegawa, K. Sato, Y. Sakaguchi, and H. Yoshinaga, "Effect of Crystal Structure on High Temperature Deformation Behaviour of Silicon Carbides", *Materials Trans., JIM*, **34**[8] (1993) 675-81.
11. B. Palosz, *et al.* "High Pressure Diffraction Studies of Flame-Generated Silicon Carbide Powders", American Ceramic Society Annual Meeting, Cincinnati, OH, May 4-7, 1997.
12. J. S. Nadeau, "Very High Pressure Hot Pressing of Silicon Carbide", *Ceramic Bulletin*, **52**[2] (1973) 170-74.
13. O. Yamada, Y. Miyamoto, and M. Koizumi, "High Pressure Self-Combustion Sintering of Silicon Carbide", *Ceramic Bulletin*, **64**[2] (1985) 319-21.
14. M. Yoshida, A. Onodera, M. Ueno, K. Takemura, and O. Shimomura, "Pressure-Induced Structure Transition in SiC", *Physical Review B*, **48**[14] (1993) 10587-90.
15. S. Stel'makh, S. Gierlotka, B. Palosz, M. Mohan, C. Divakar, S. K. Baumik, and A. K. Singh, "Effect of High Pressure on Polytypism and Stacking Disorder in Sintered SiC", *XXIII IUCrystallography Congress*, Seattle, USA (1996).
16. B. Palosz, S. Stel'makh, and S. Gierlotka, "Refinement of Polycrystalline Disordered Cubic Silicon Carbide by Structure Modeling and X-ray Diffraction Simulation", *Zeitschrift fur Kristallographie*, **210** (1995) 731-40.
17. W. Rafaniello, K. Cho and A. V. Virkar, *J. Mater. Sci.*, **16** (1981) 3479-3488.
18. W. R. Schmidt, L. V. Interrante, R. H. Doremus, T. K. Trout, P. S. Marchetti and G. E. Maciel, *Chem. Mater.*, **3** (1991) 257-267.
19. C. Czekaj, M. L. J. Hackney, W. J. Hurley, Jr., L. V. Interrante, G. A. Sigel, P. J. Shields, and G. A. Slack, *J. Am. Ceram. Soc.*, **73**[2] 1990 352-357.
20. W. R. Schmidt, W. J. Hurley, Jr., R. H. Doremus, L. V. Interrante, and P. S. Marchetti, *Advanced Composite Materials; Ceramic Transactions 19*, M. D. Sacks, editor; American Ceramic Society: Westerville, OH, (1991) pp. 19-25.

21. J. F. Janik, E. N. Duesler and R. T. Paine, *Inorg. Chem.*, **26** (1987) 4341-4345.
22. R. T. Paine, J. F. Janik, C. Narula, *Mater. Res. Soc. Symp. Proc.*, **121** (1988) 461-464.
23. A. Zangvil and R. Ruh, *J. Am. Ceram. Soc.*, **71**[10] (1988) 884-90.

## 5.0 ACKNOWLEDGMENTS

The author thanks Dr. Bruce Laube (UTRC) and Mr. Jack Knecht (UTRC) for acquiring some of the X-ray powder diffraction data collected during this program; Mr. Mark Hermann (UTRC) for preparation of all polymers, polymer blends, and heat treated samples; Mr. Laurence Pryor (UTRC) for thermal analysis experiments; and Mr. Gerald McCarthy (UTRC) for TEM evaluation of the nanocrystalline ceramic samples.

Solid-state NMR spectra were obtained at Rensselaer Polytechnic Institute by Dr. Sanlin Hu, Ms. Giselle Verdecia, and Ms. Kerry O'Brien under the direction of Professor Thomas Apple, and funded, in part, by the National Science Foundation under grant CHE-9520930.

Some of the TEM analysis and densification experiments on the polymer-derived ceramics were performed at Rutgers University by Drs. Gang Qi and Chid Kallingal under the direction of Professor Stephen Danforth.

High pressure and high temperature diffraction studies were performed under the direction of Professor Bogdan. Palosz at the High Pressure Research Center (UNIPRESS) in Warsaw, Poland, with sponsorship from the State Committee for Scientific Research, Grants P40708906 and 7 T08 A026 11, and supported by BMPF, Germany, under Contract No. POL-153-97. Experiments at HASYLAB (DESY in Hamburg, Germany) were performed on project II-95-15 by P. Zinn. Preparation of nanocrystalline SiC AeroChem was performed by Dr. David Keil and partially supported by the National Science Foundation under Grant 9320599.

Dr. Alexander Pechenik at AFOSR is acknowledged for this program's sponsorship.

## 6.0 PERSONNEL SUPPORTED

The following personnel were supported, in part, during the contract period of performance.

### 6.1 United Technologies Research Center

Dr. Wayde R. Schmidt (Principal Investigator)  
Dr. Bruce Laube

Mr. Jack Knecht  
Mr. Gerald McCarthy  
Mr. Mark Hermann  
Mr. Laurence Pryor

## **6.2 Rutgers, The State University of New Jersey**

Dr. Stephen C. Danforth (Faculty Member)  
Dr. Chid Kallingal (Postdoctoral Researcher)  
Dr. Gang Qi (Postdoctoral Researcher)

## **6.3 Rensselaer Polytechnic Institute**

Dr. Thomas Apple (Faculty Member)  
Dr. Sanlin Hu (Postdoctoral Researcher)  
Ms. Gissel Verdecia (Graduate Student)  
Ms. Kerry O'Brien (Undergraduate Student)

# **7.0 PUBLICATIONS AND PRESENTATIONS**

The following publications were supported, fully or in part, by Contract No. F49620-95-0020:

"Aluminum-27 and Silicon-29 Solid-State Nuclear Magnetic Resonance Study of Silicon Carbide/Aluminum Nitride Systems: Effect of Silicon/Aluminum Ratio and Pyrolysis Temperature", G. Verdecia, K. L. O'Brien, W. R. Schmidt, and T. M. Apple, *Chem. Mater.* (1998), **10**[4] 1003-1009.

"Microstructural Evaluation of Sintered Nanoscale SiC Powders Prepared by Various Processing Routes", W. R. Schmidt, G. McCarthy, B. Palosz, S. Stel'makh, M. Aloshina, S. Gierlotka, P. Zinn, D. G. Keil, H. F. and Calcote, *Mat. Res. Soc. Symp. Proc.* (1998) **501**, 21-26.

A paper entitled "Development of Poly(methylvinylsilane) Blends for Matrix Applications in Ceramic Matrix Composites", Wayde R. Schmidt, John P. Wesson, Sanlin Hu, Thomas Apple, Howard B. Jones, and Wilson Horne was prepared for submission to *Chemistry of Materials*, and is awaiting legal review at UTRC.

"Poly(borosilazane) Precursors to Ceramic Nanocomposites", Wayde R. Schmidt, D. M. Narsavage-Heald, D. M. Jones, P. S. Marchetti, D. Raker, and G. Maciel; accepted for publication in *Chemistry of Materials* (Sept. 1998).

The following presentations were supported, fully or in part, by Contract No. F49620-95-0020:



May 23-24, 1995: W. Schmidt presented a poster entitled "Silicon-Based Nanostructural Ceramics Derived From Polymer Precursors: Development of Processing, Structure & Property Relationships" at the AFOSR Annual Contract Review at Hueston Woods.

March 28, 1996: W. Schmidt presented an invited seminar entitled "Silicon-Based Non-Oxide Ceramics from Polymer Precursors" at the University of New Hampshire, Durham, NH.

April 14-17, 1996: W. Schmidt presented two papers at the National Meeting of the American Ceramic Society in Indianapolis. The papers were entitled (1) "Polymer Precursor Blends for Nonoxide Nanostructured Ceramics", and (2) Nanostructured SiC/AlN Solid Solutions via Preceramic Polymers".

October 31, 1996: G. Verdecia presented her Ph.D. thesis research work on the solid state NMR of SiC/AlN precursor system at the Rensselaer Polytechnic Institute Department of Chemistry seminar.

May 6, 1997: W. Schmidt presented a poster entitled "High Pressure, High Temperature Diffraction Studies of Silicon Carbide Prepared from Polymer Precursors" at the American Ceramic Society Annual Meeting in Cincinnati, OH.

May 8-9, 1997: W. Schmidt presented a summary of the previous year's accomplishments at the annual AFOSR Contractor's review in Cincinnati, OH.

May 14, 1997: W. Schmidt presented an invited seminar at the University of Connecticut's Institute of Materials Science, Department of Metallurgy, entitled "Si-Based Nanostructural Ceramics Derived from Polymer Precursors".

June 24, 1997: G. Verdecia presented an update on her Ph.D. thesis research on the solid state NMR of SiC/AlN precursor system at the Northeast Regional Meeting of the American Chemical Society (NERM '97).

October 14, 1997: W. Schmidt presented a paper entitled "Nanostructured Non-Oxide Ceramics via Polymeric Precursors" at the Pacific Coast Regional and Basic Science Divisional Meeting of the American Ceramic Society in San Francisco, CA.

October 14, 1997: W. Schmidt was a co-author on a paper entitled "Poly(borosilazane) Precursors to Ceramic Nanocomposites" at the Pacific Coast Regional and Basic Science Divisional Meeting of the American Ceramic Society in San Francisco, CA.

November 16-21, 1997: G. Verdecia presented a paper entitled "<sup>27</sup>Al and <sup>29</sup>Si Solid State NMR Study of SiC/AlN Systems: Effects of Si(N)/Al Ratio and Pyrolysis Temperature" at the Eastern Analytical Symposium in Somerset, NJ.



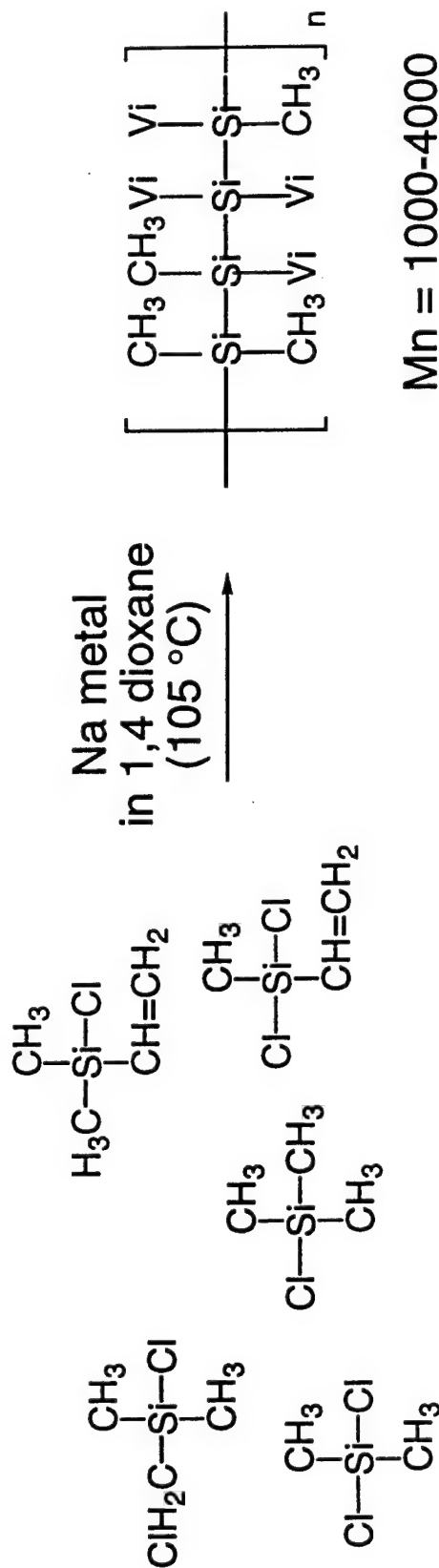
December 1, 1997: W. Schmidt presented a paper, entitled "Microstructural Evaluation of Sintered SiC Prepared by Various Processing Routes", at the Materials Research Society Annual Fall Meeting in Boston, MA.

December 3, 1997: W. Schmidt was a co-author on a paper presented by Professor B. Palosz (Unipress), entitled "Modeling of Strain Distribution in Non-Hydrostatically Pressed Nanocrystalline SiC; In-situ X-ray Diffraction Study", at the Materials Research Society Annual Fall Meeting in Boston, MA.

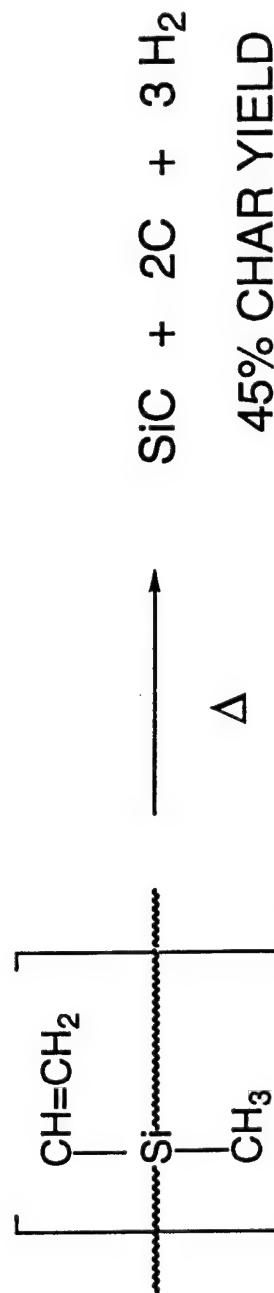
# SILICON CARBIDE SOURCE

## *POLY(METHYL VINYLSILANE)*

### *Polymer Synthesis*



### *Polymer Pyrolysis and Conversion*



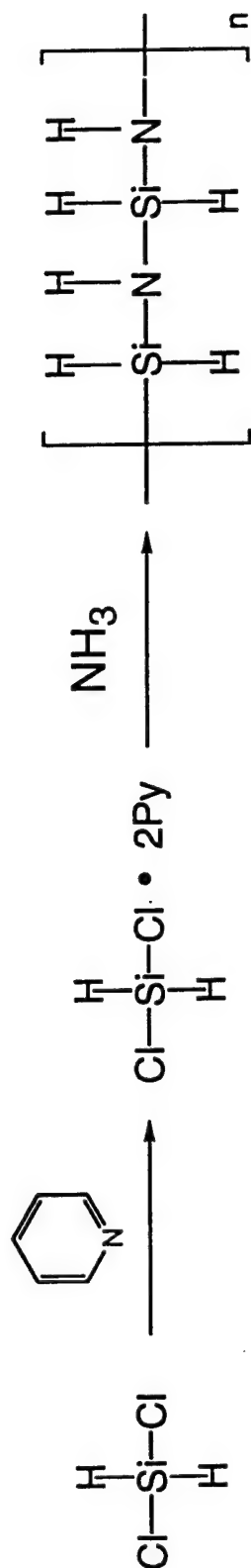
UNITED  
TECHNOLOGIES  
RESEARCH  
CENTER

FIGURE 1

# SILICON NITRIDE SOURCE

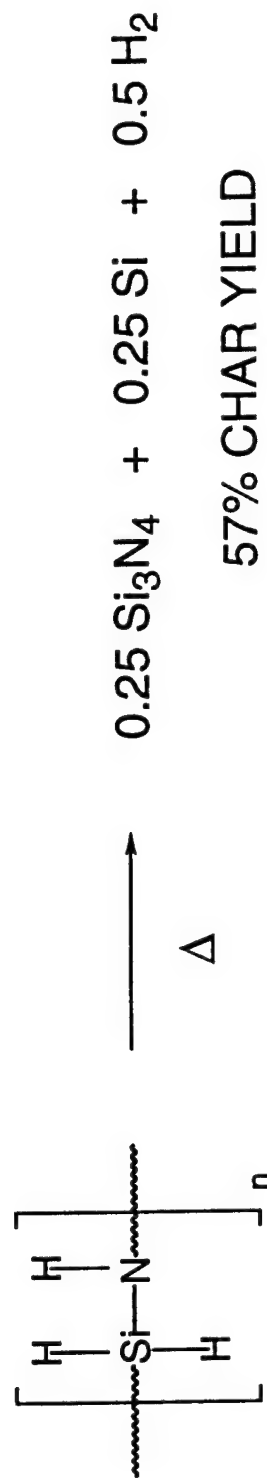
## PERHYDRIDOPOLY(SILAZANE) (TONEN PHPS)

### Polymer Synthesis



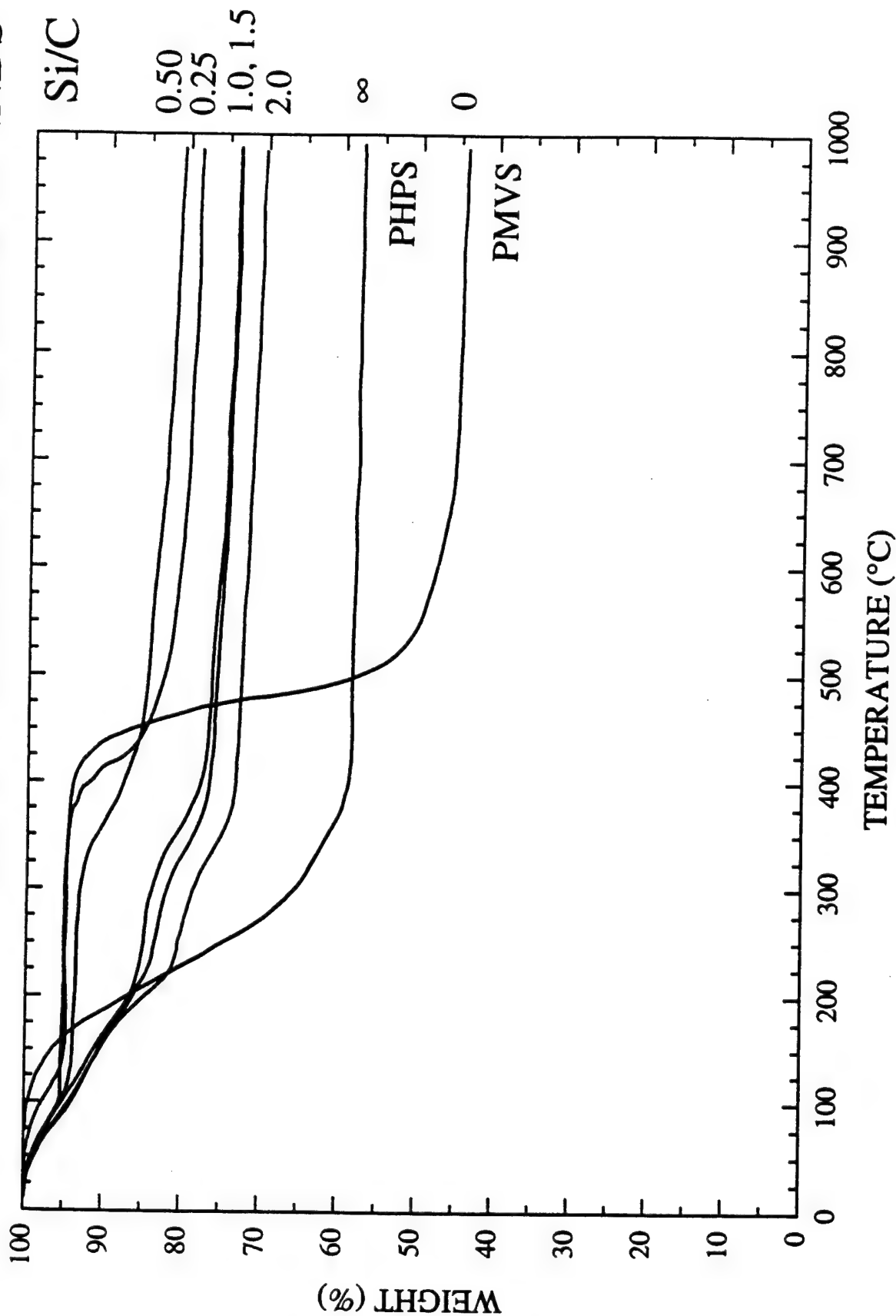
$M_n = 1000-4000$

### Polymer Pyrolysis and Conversion

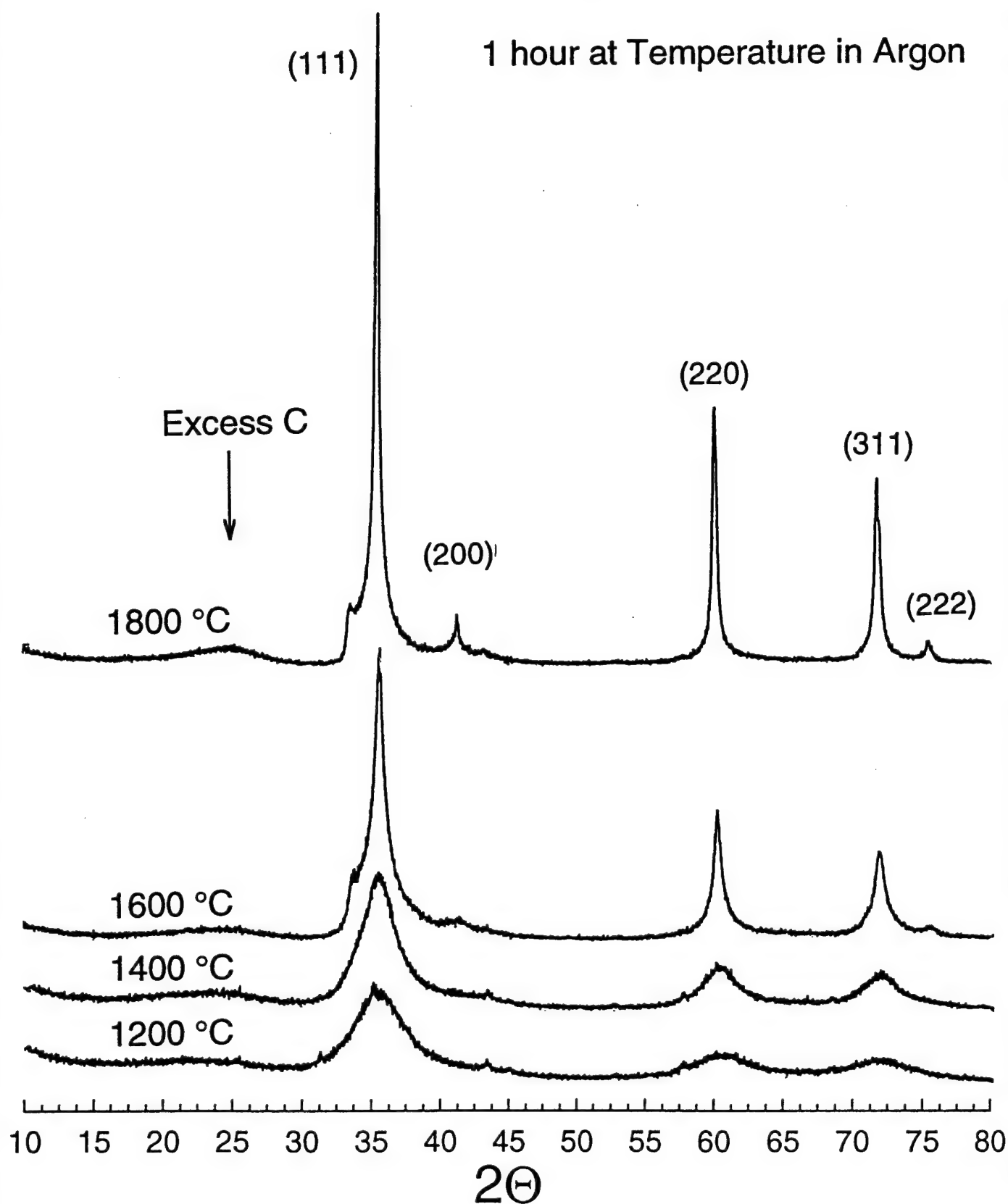


57% CHAR YIELD

# THERMAL ANALYSIS OF PHPS/PMVS POLYMER BLENDS



# X-ray Diffraction Patterns of PMVS Only



# Effect of Time and Temperature on Grain Size in PMVS Char

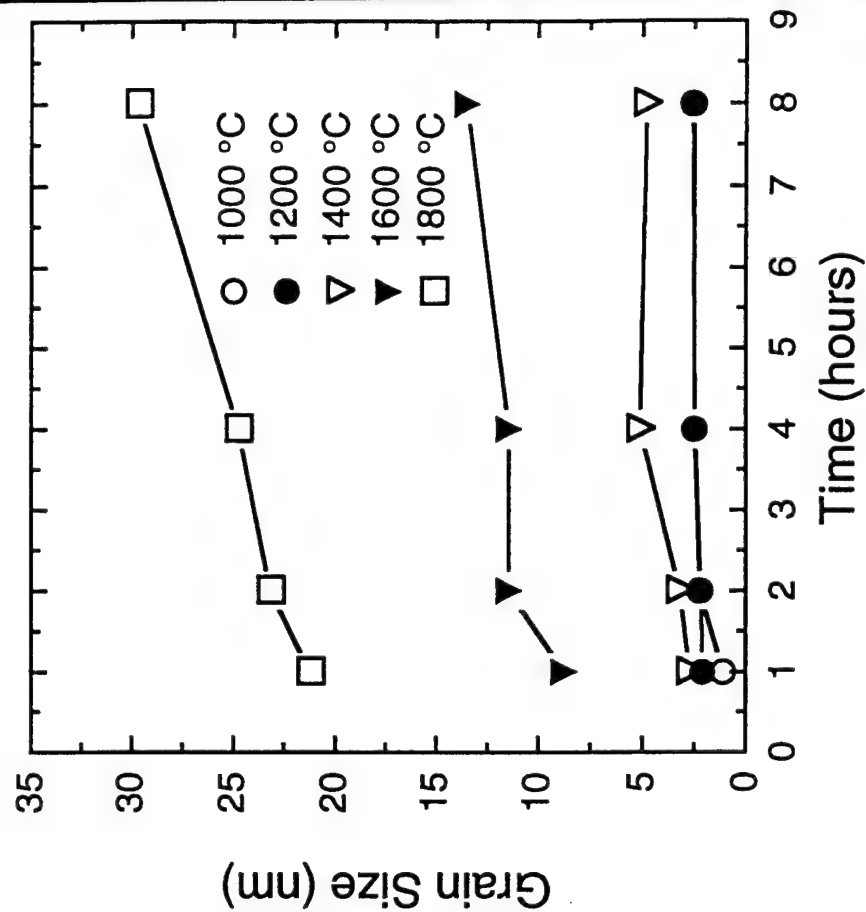
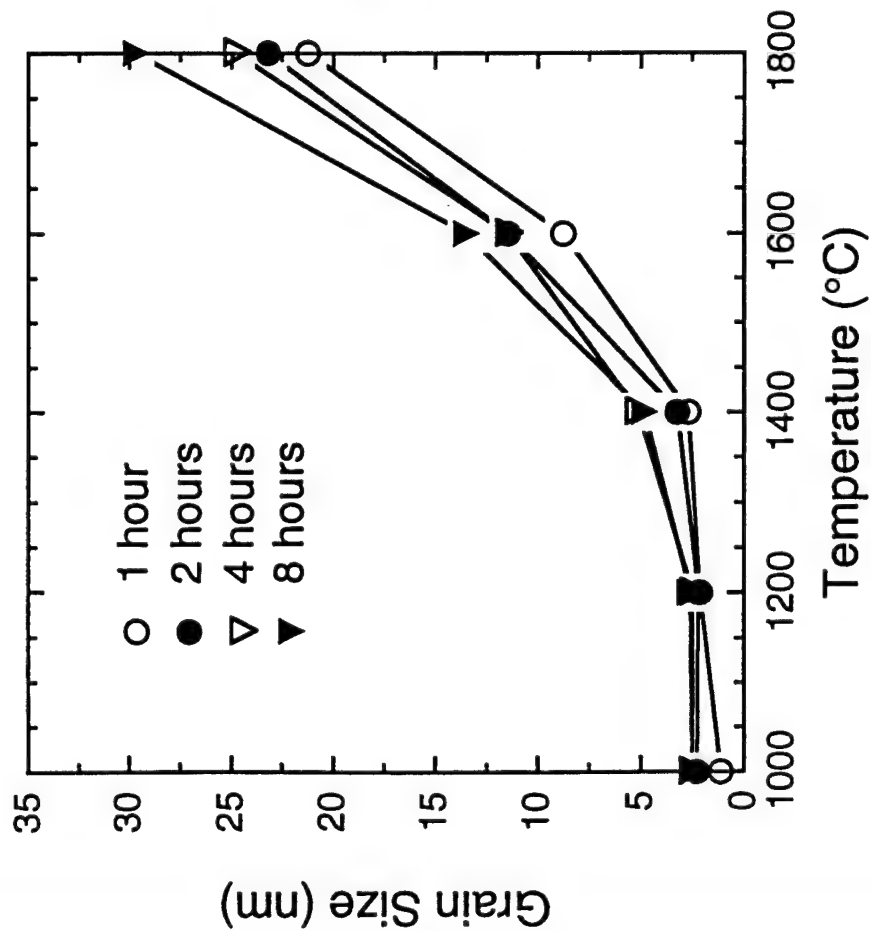
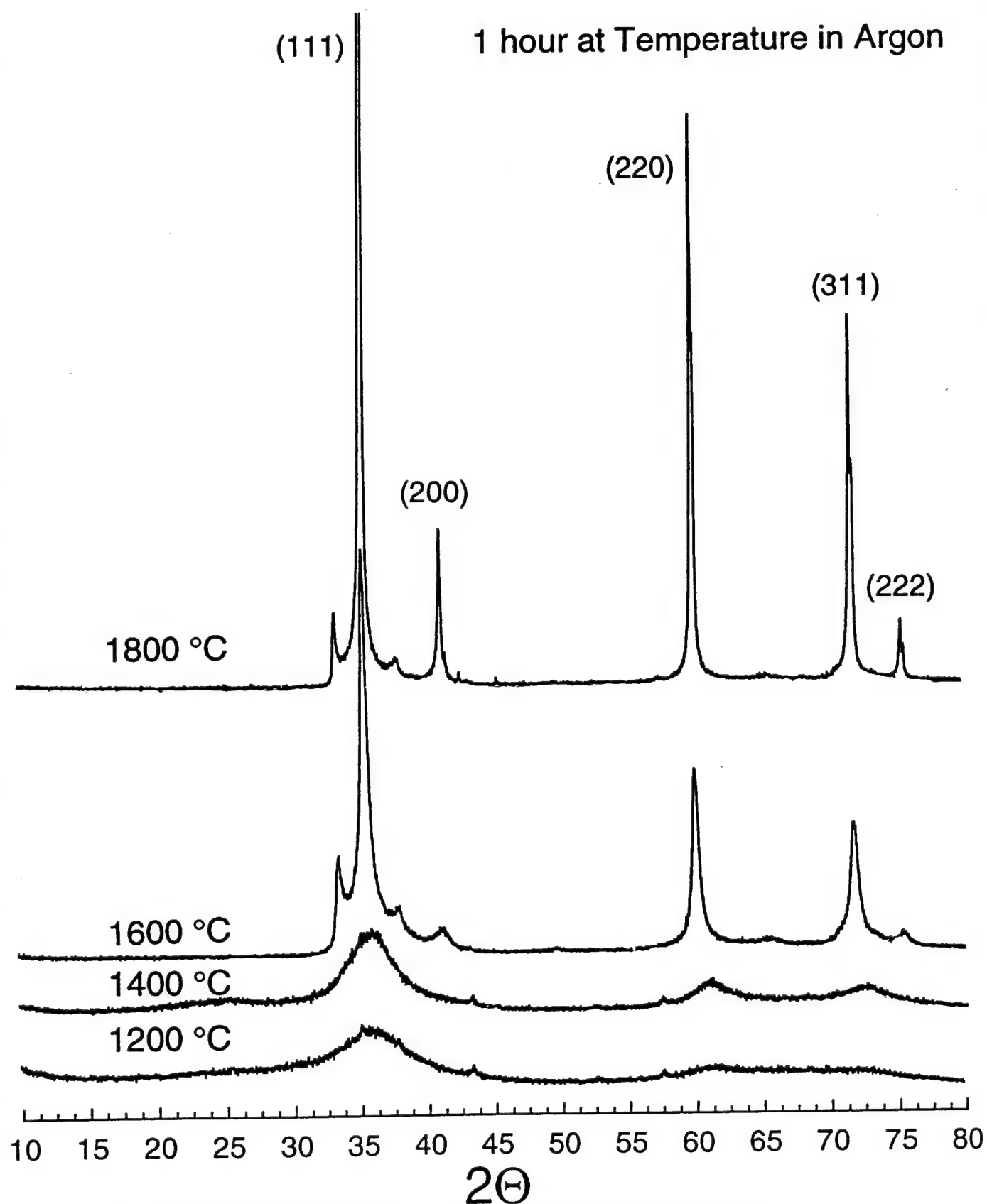


FIGURE 6

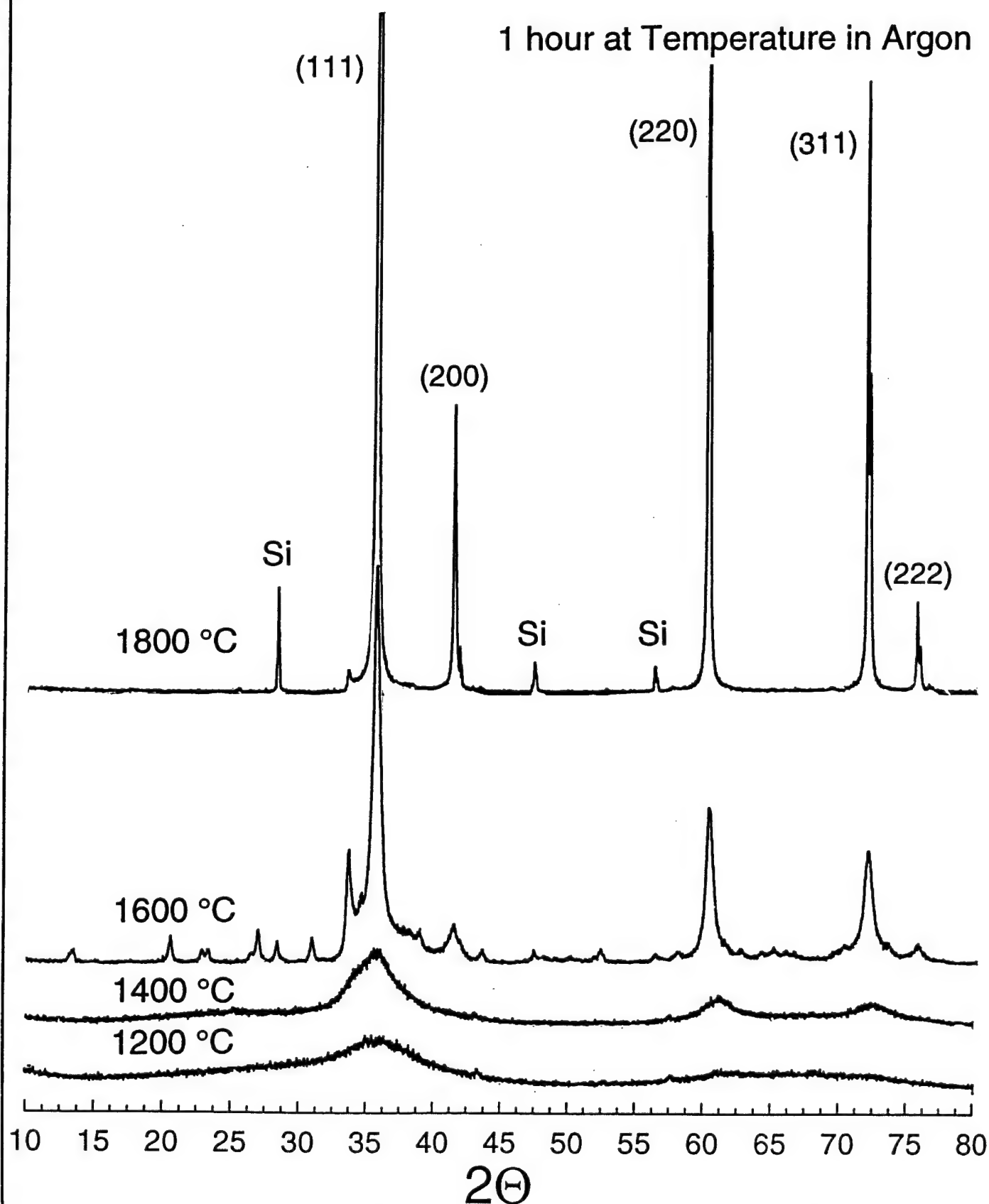
# X-ray Diffraction Patterns of PMVS/PHPS Blend B, Si/C=0.25

1 hour at Temperature in Argon



# X-ray Diffraction Patterns of PMVS/PHPS Blend C, Si/C=0.5

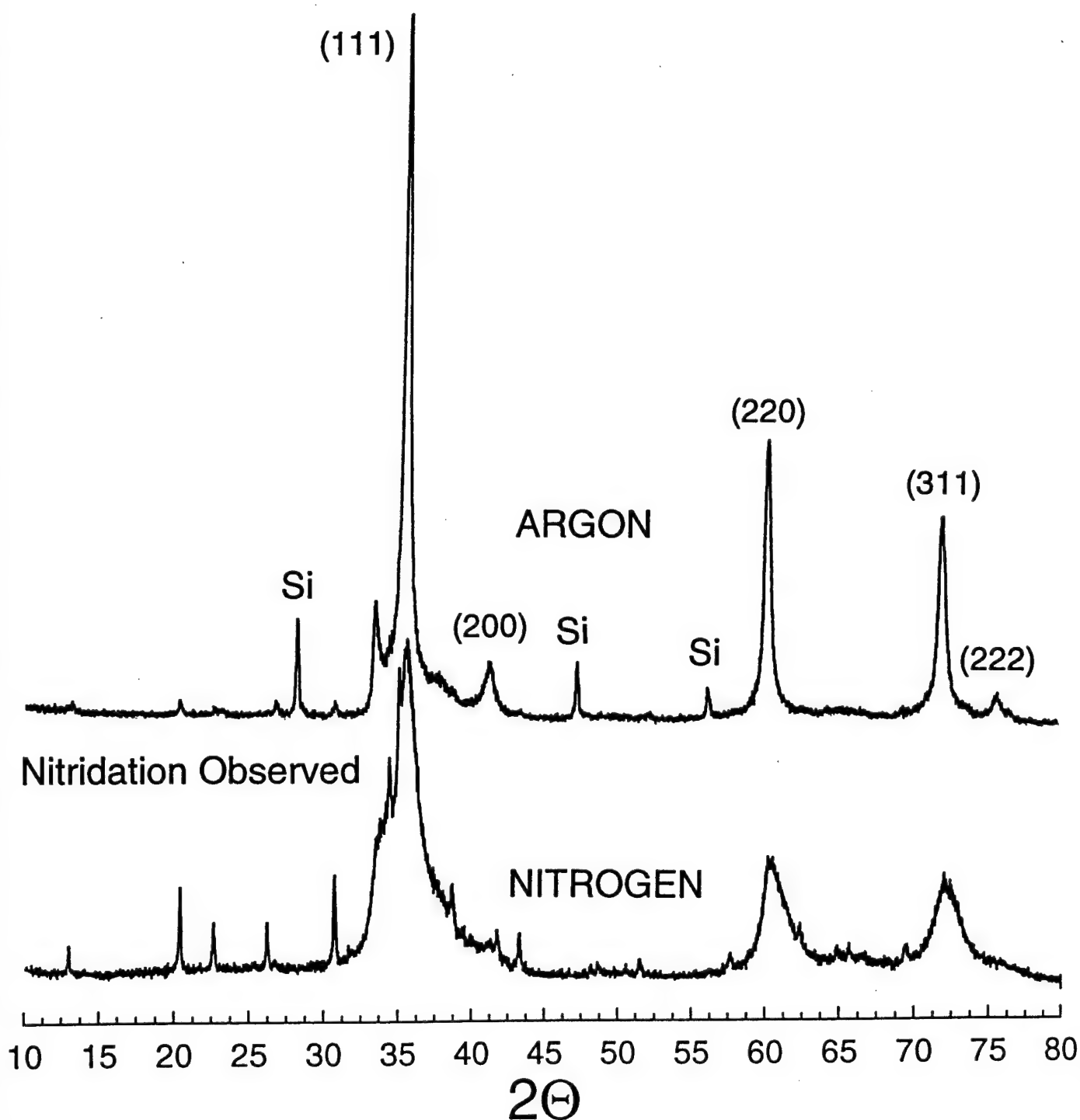
1 hour at Temperature in Argon





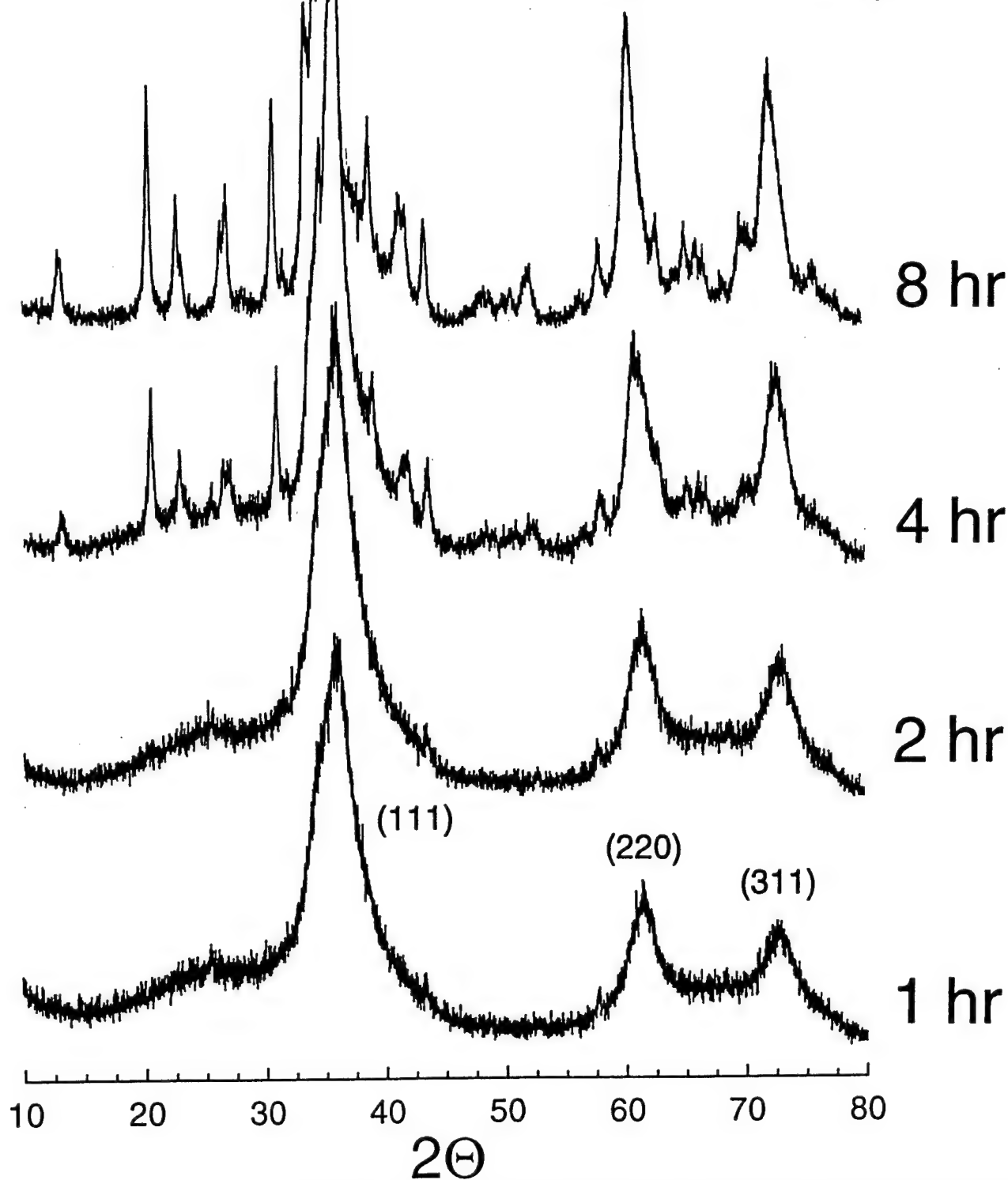
# X-ray Diffraction Patterns of PMVS/PHPS Blend C, Si/C=0.5

2 hours at 1600 °C



# X-ray Diffraction Patterns of PMVS/PHPS Blend C, Si/C=0.5

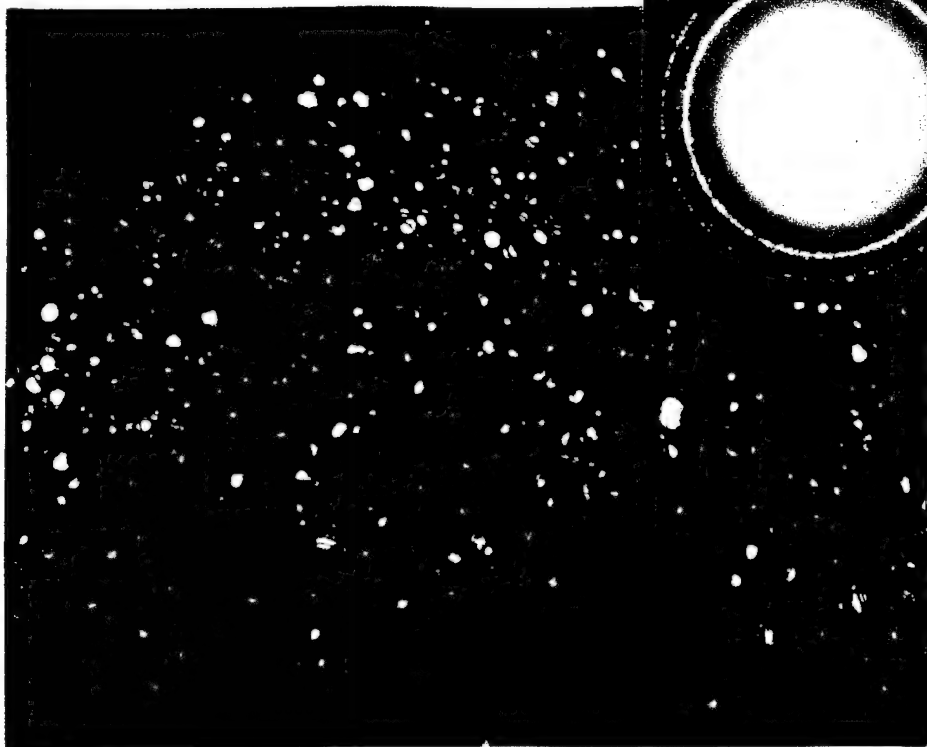
1400 °C in Argon



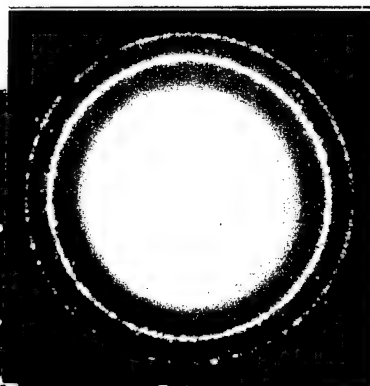
# TEM/SAED OF PHPS/PMVS BLENDS

1600 °C

Si/C = 0

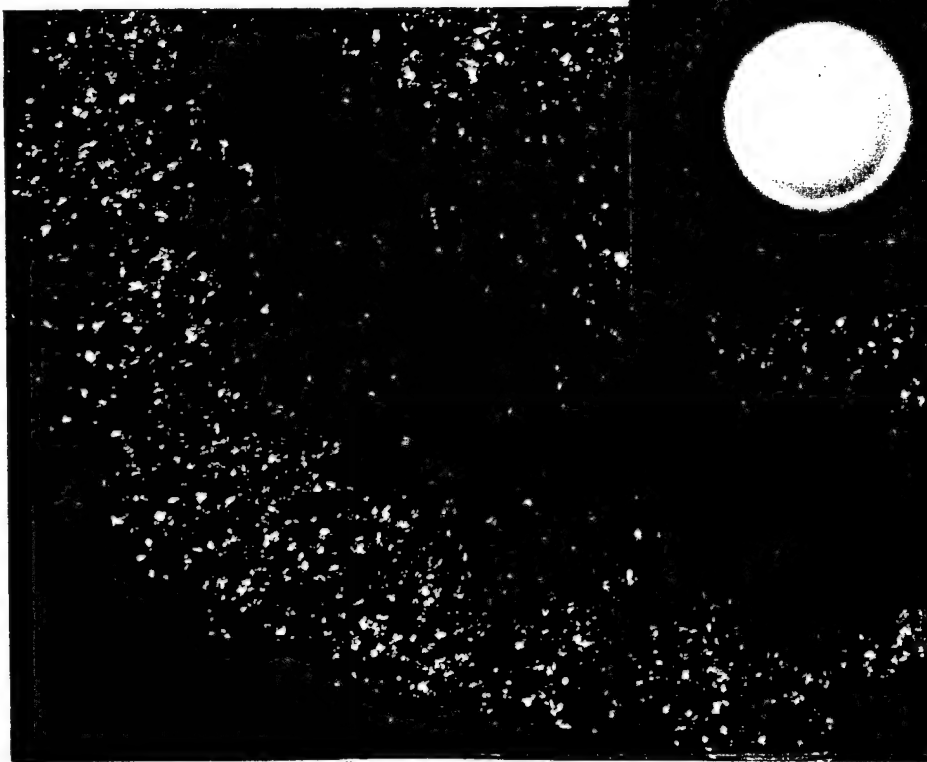


DARK FIELD

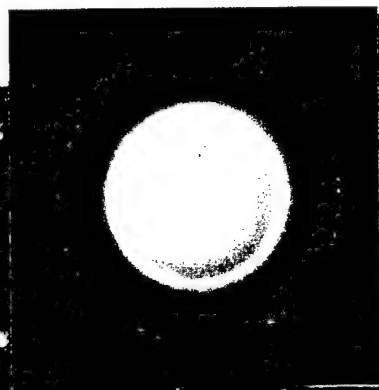


SiC

Si/C = 1.0



DARK FIELD



SiC + Si<sub>3</sub>N<sub>4</sub>



100 nm

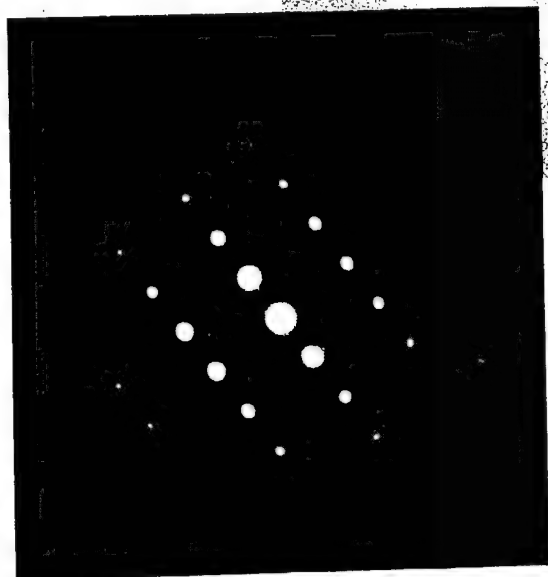


UNITED  
TECHNOLOGIES  
RESEARCH  
CENTER

FIGURE 10

**TEM Micrograph of PMVS/PHPS Blend C**  
**( $x_s \text{ Si}/x_s \text{ C} = 0.5$ ) Heated at  $1400^\circ\text{C}$  for 2 hours in Ar**

SiC Whisker



120 nm



UNITED  
TECHNOLOGIES  
RESEARCH  
CENTER

TEM Micrographs of PMVS/PHPS Blend C (xs Si/xs C = 0.5)  
Heated at 1600°C for 2 hours in Ar

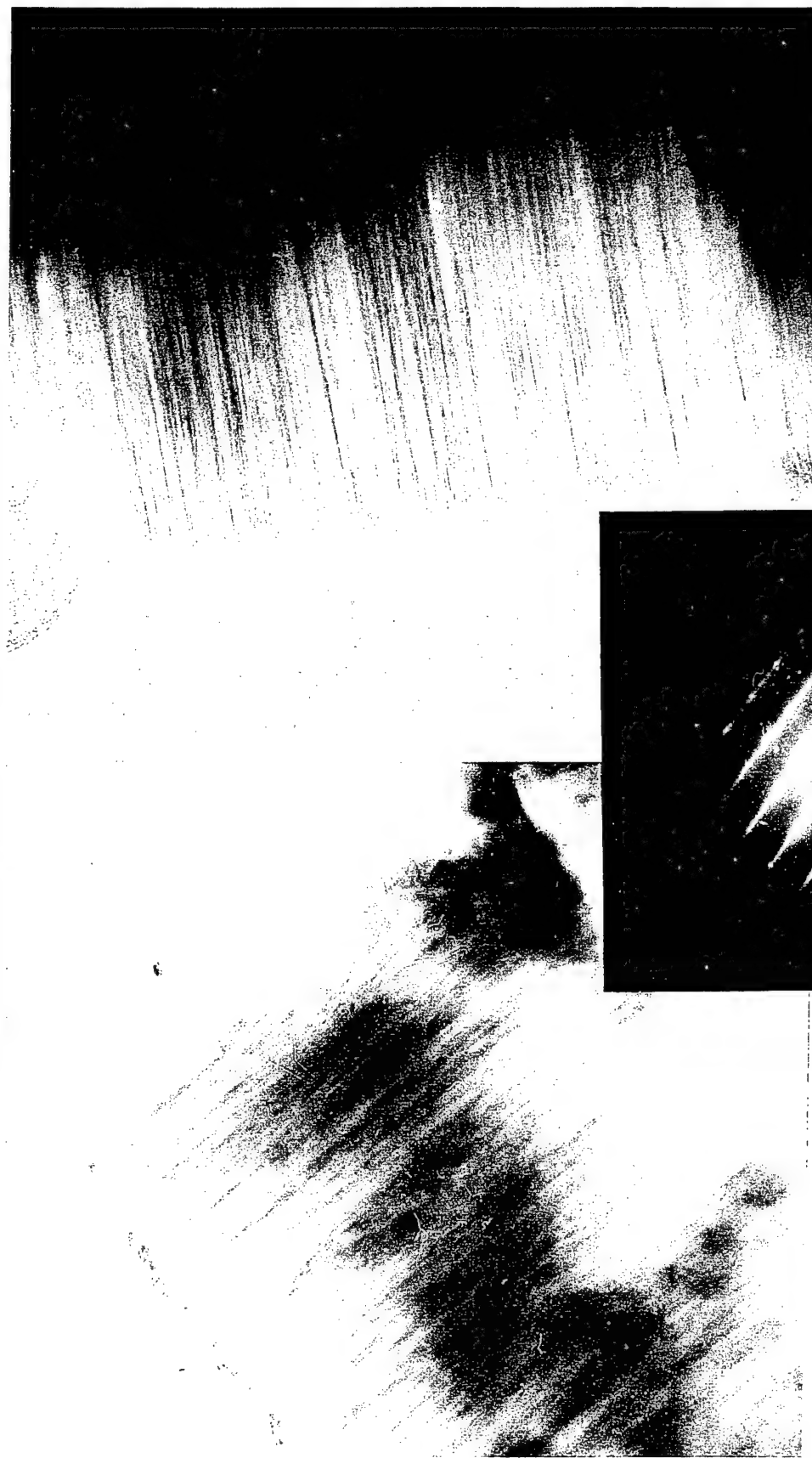
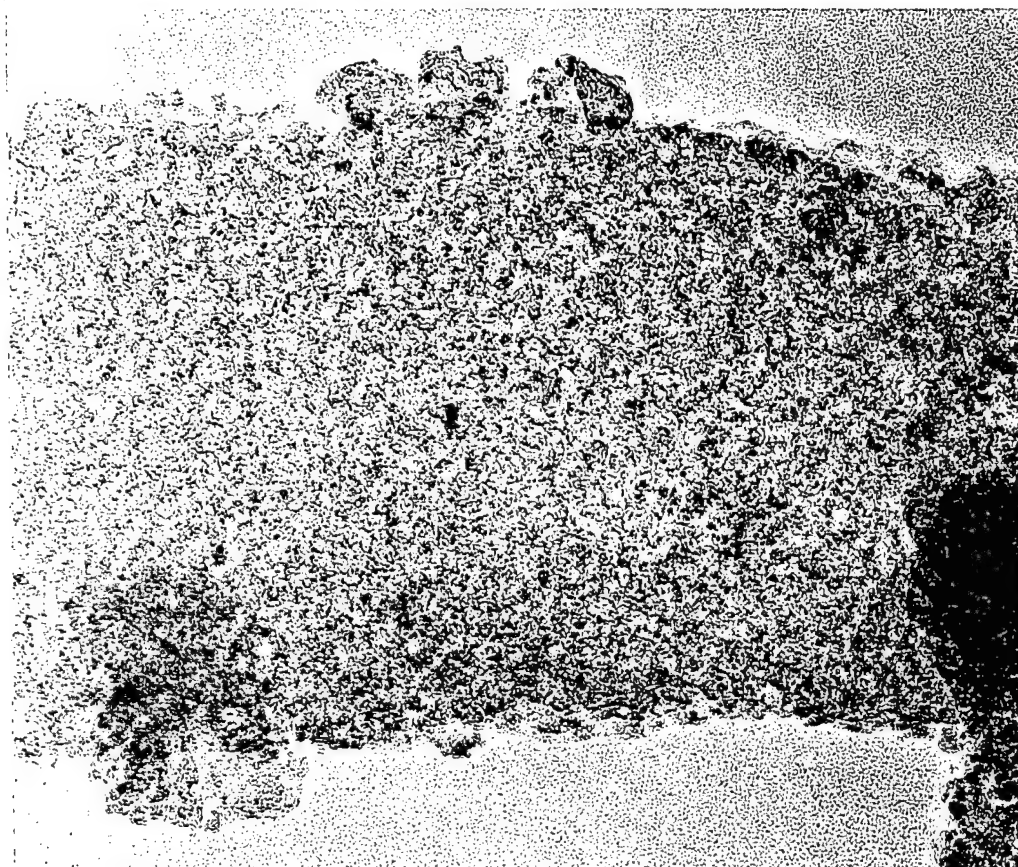


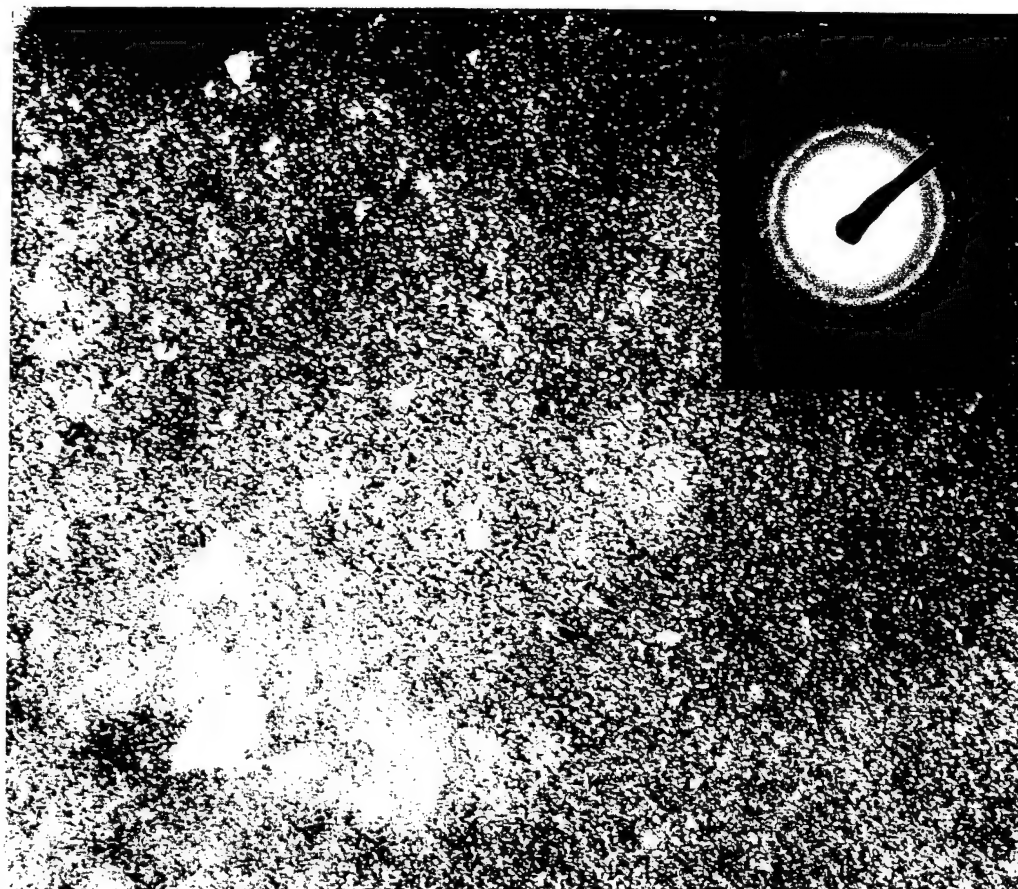
FIGURE 12

SiC Whisker

**TEM Micrographs of PMVS/PHPS Blend C (xs Si/xs C = 0.5)  
Heated at 1400°C for 2 hours in Ar**



SiC



100 nm



UNITED  
TECHNOLOGIES  
RESEARCH  
CENTER

25 nm



**TEM Micrographs of PMVS/PHPS Blend C ( $x_s$  Si/ $x_s$  C = 0.5)  
Heated at 1400°C for 4 hours in Ar**

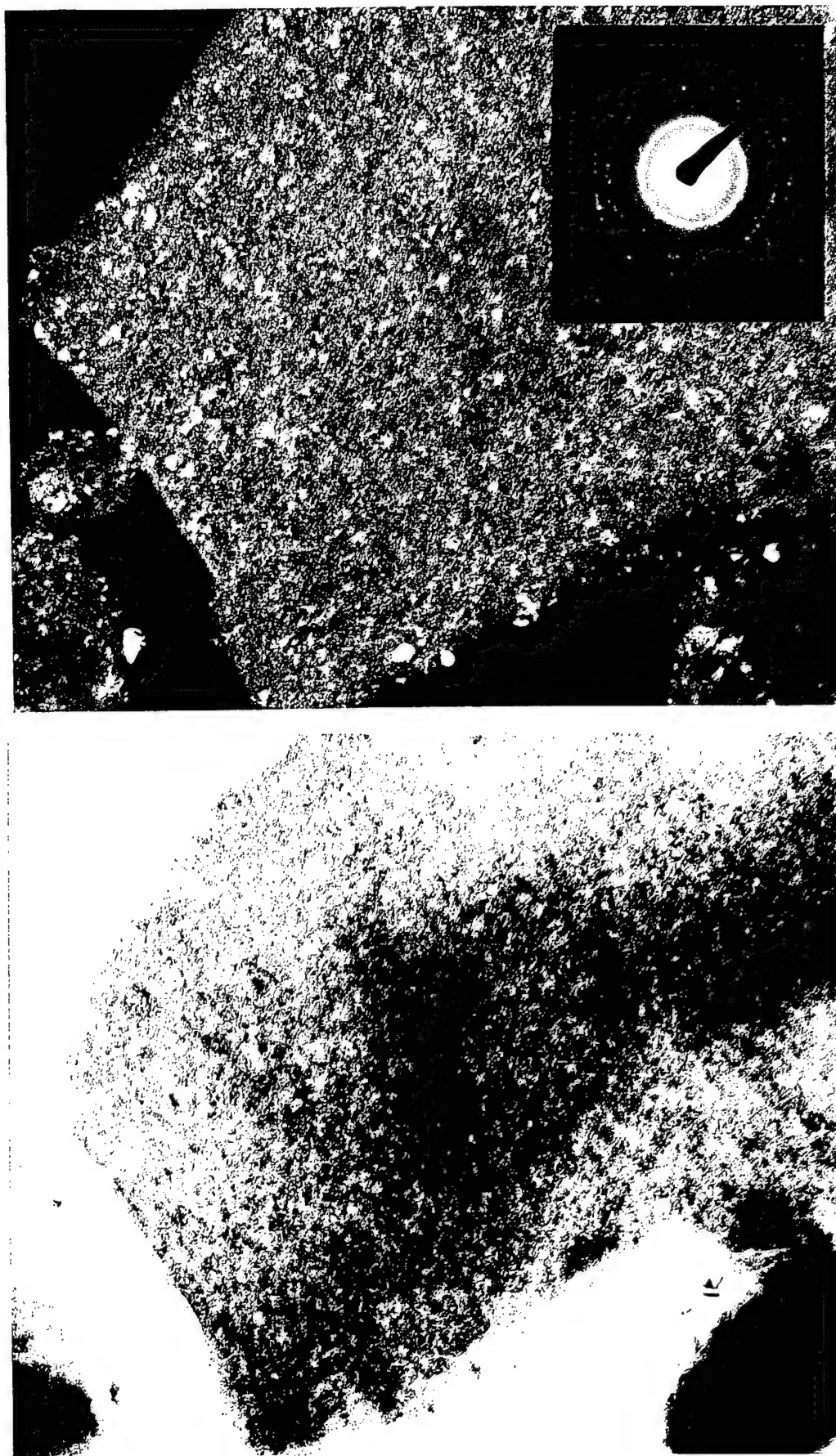


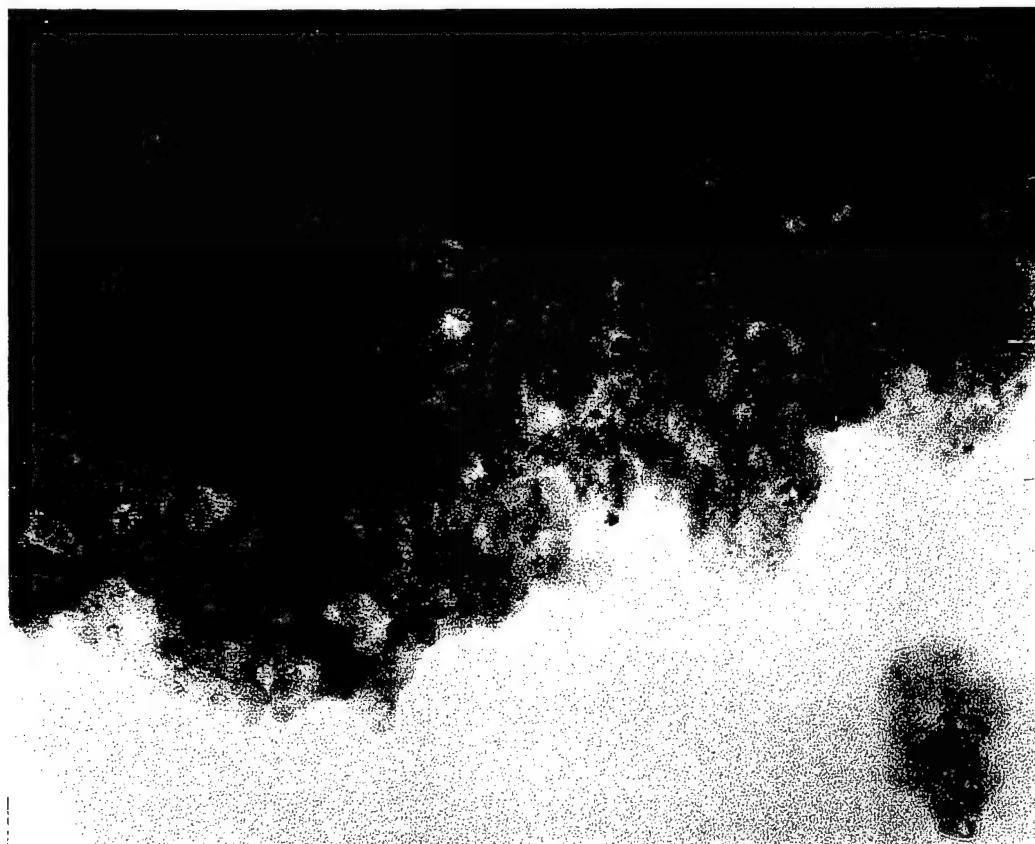
FIGURE 14

SiC

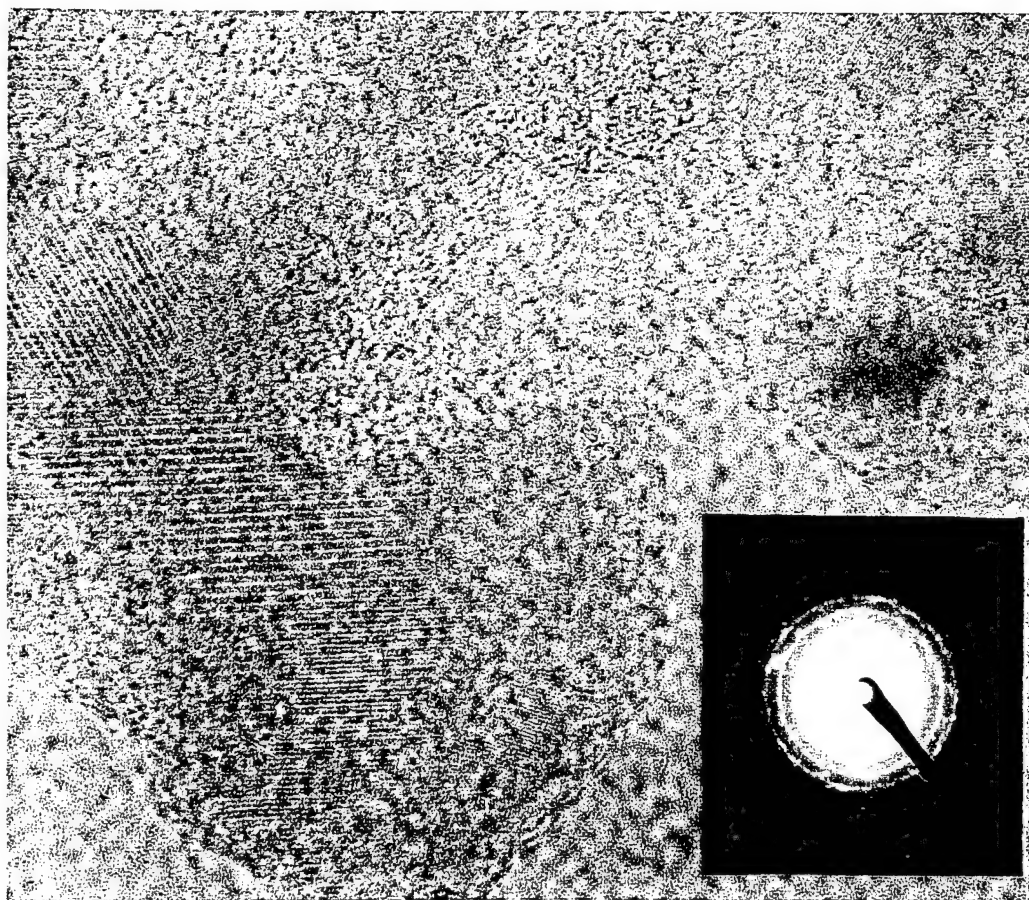


UNITED  
TECHNOLOGIES  
RESEARCH  
CENTER

# TEM Micrographs of PMVS/PHPS Blend C (xs Si/xs C = 0.5) Heated at 1400°C for 4 hours in Ar



100 nm



SiC plus  $\alpha$ -Si<sub>3</sub>N<sub>4</sub>  
(100) 0.671 nm lattice

10 nm



UNITED  
TECHNOLOGIES  
RESEARCH  
CENTER

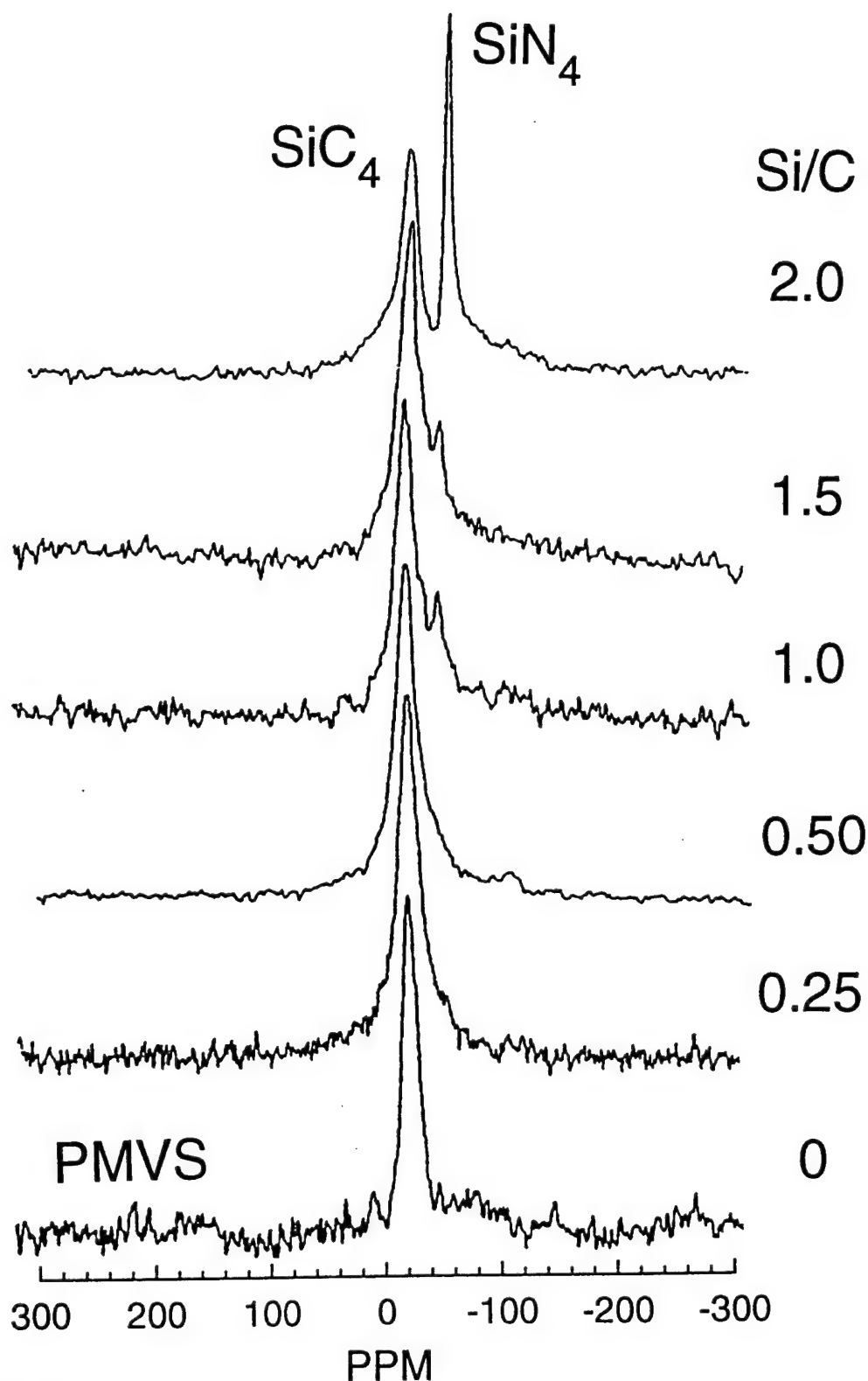


TEM Micrographs of PMVS/PHPS Blend C (xs Si/xs C = 0.5)  
Heated at 1400°C for 8 hours in Ar



# Solid-state $^{29}\text{Si}$ MAS NMR Spectra of PMVS/PHPS Blends

(Samples Heated Briefly to 1600 °C in Argon)



# Pellet Processing Procedure

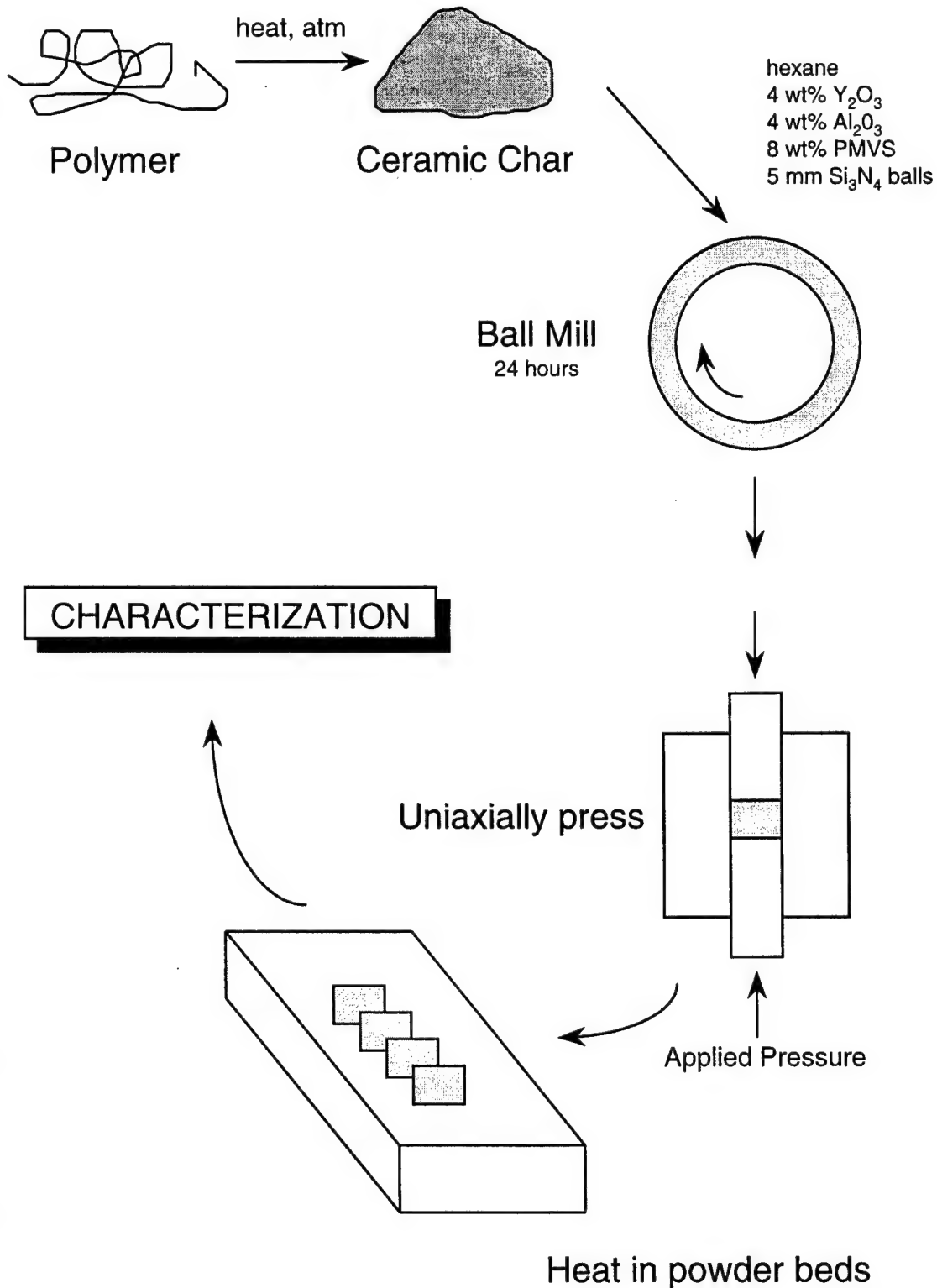


FIGURE 19

### Effect of Applied Pressure on Pellet Density

*Pellets were fabricated using Carbogran UF 15 with 8 wt% PMVS as binder*

*Pressure was applied uniaxially for 1 minute, and resulting*

*pellets were pyrolyzed in Argon to 1000 °C for 1 hour*

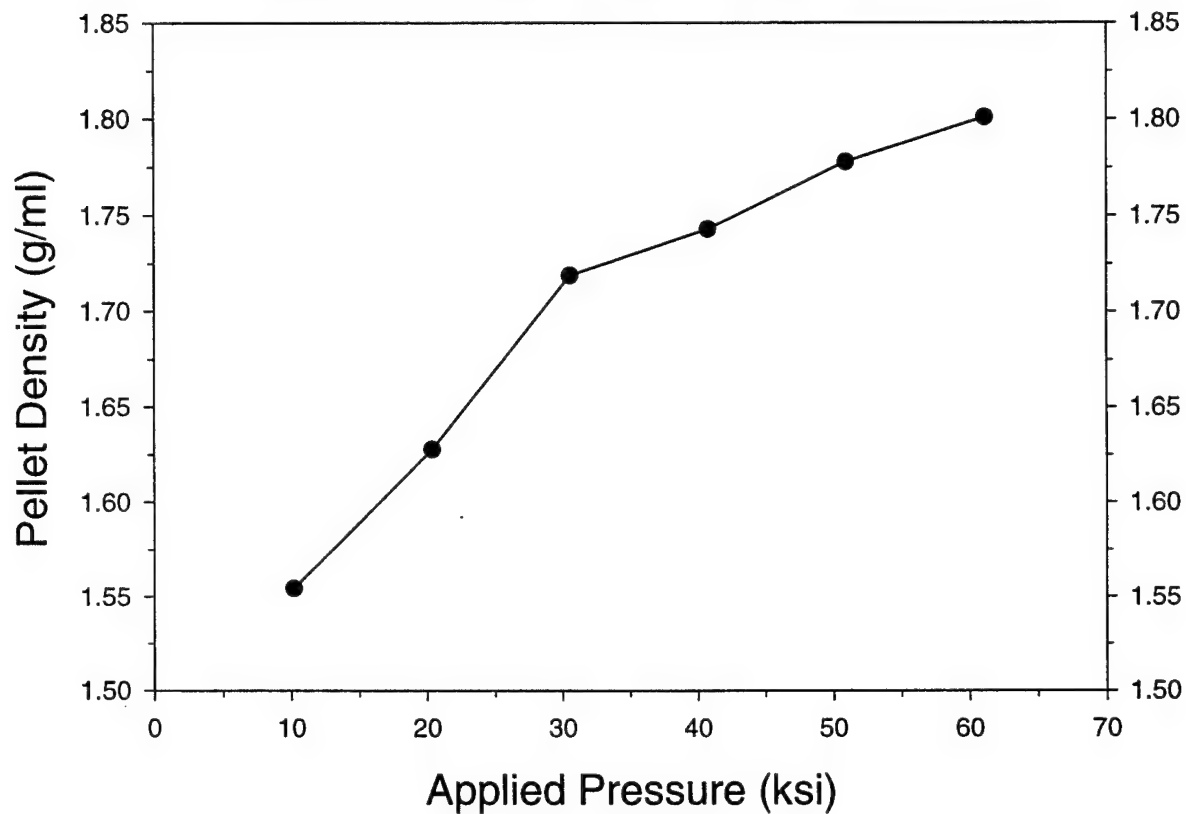
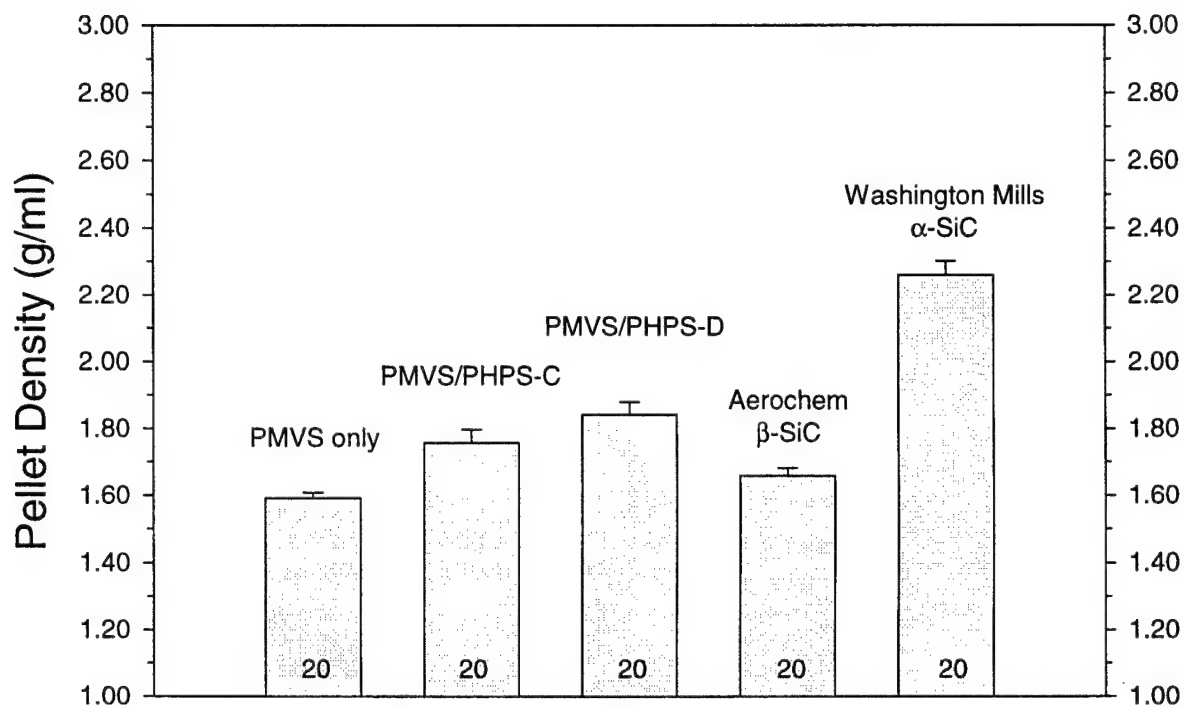


FIGURE 20

### Effect of Starting Composition on As-Processed Pellet Density



Pellets Uniaxially Pressed at 60 ksi for 1 min  
and Pyrolyzed at 1000 °C in Argon for 1 hour

FIGURE 21

PMVS only  
2 hr firing at Temperature

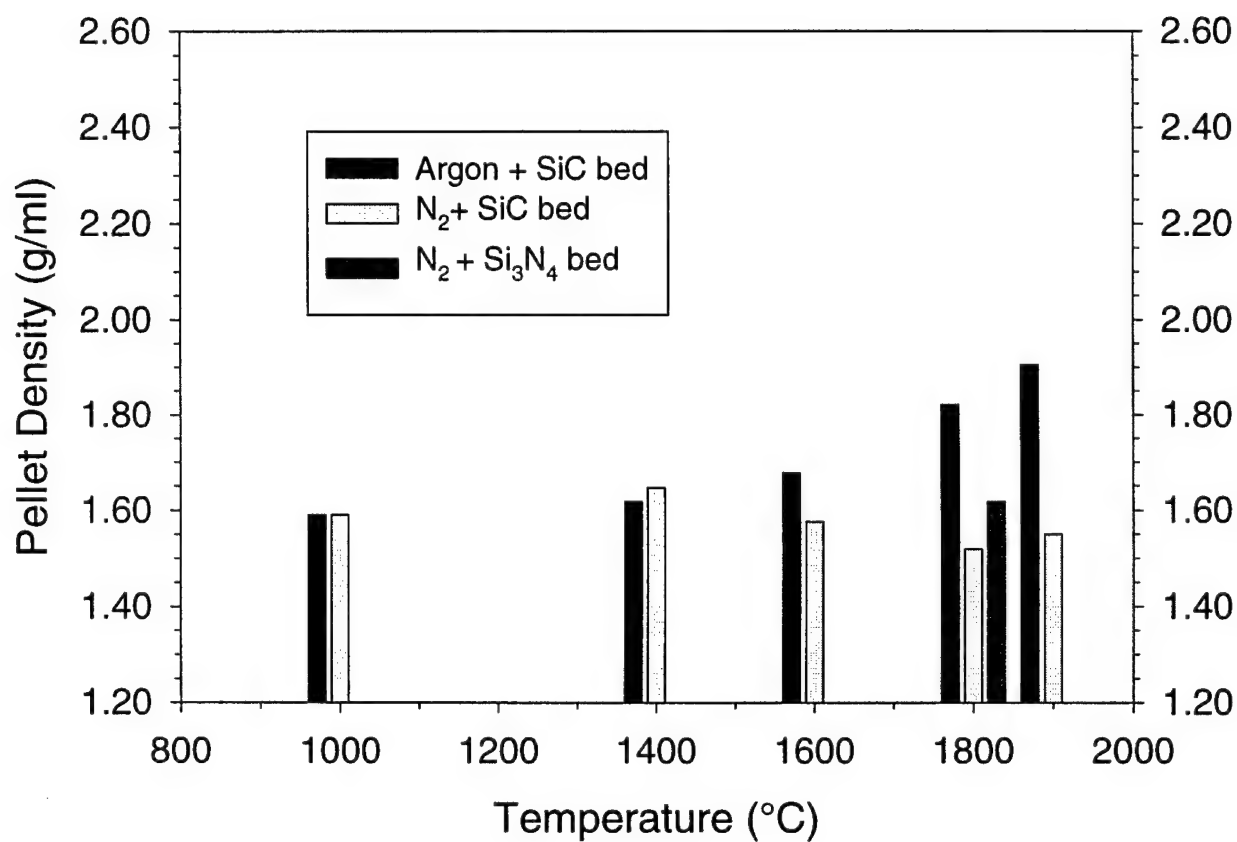


FIGURE 22

PMVS/PHPS-C (xs Si/xs C = 0.5)  
2 hr firing at Temperature

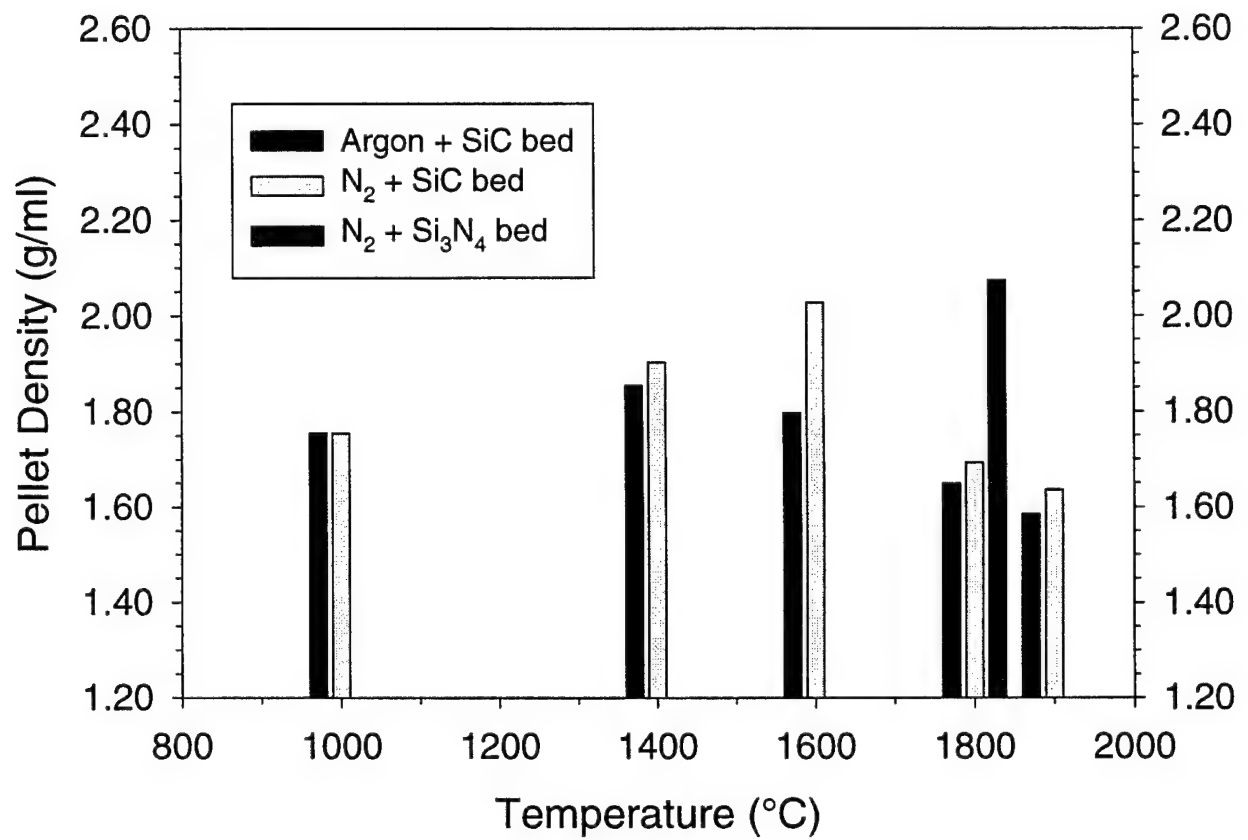


FIGURE 23

PMVS/PHPS-D (xs Si/xs C = 1)  
2 hr firing at Temperature

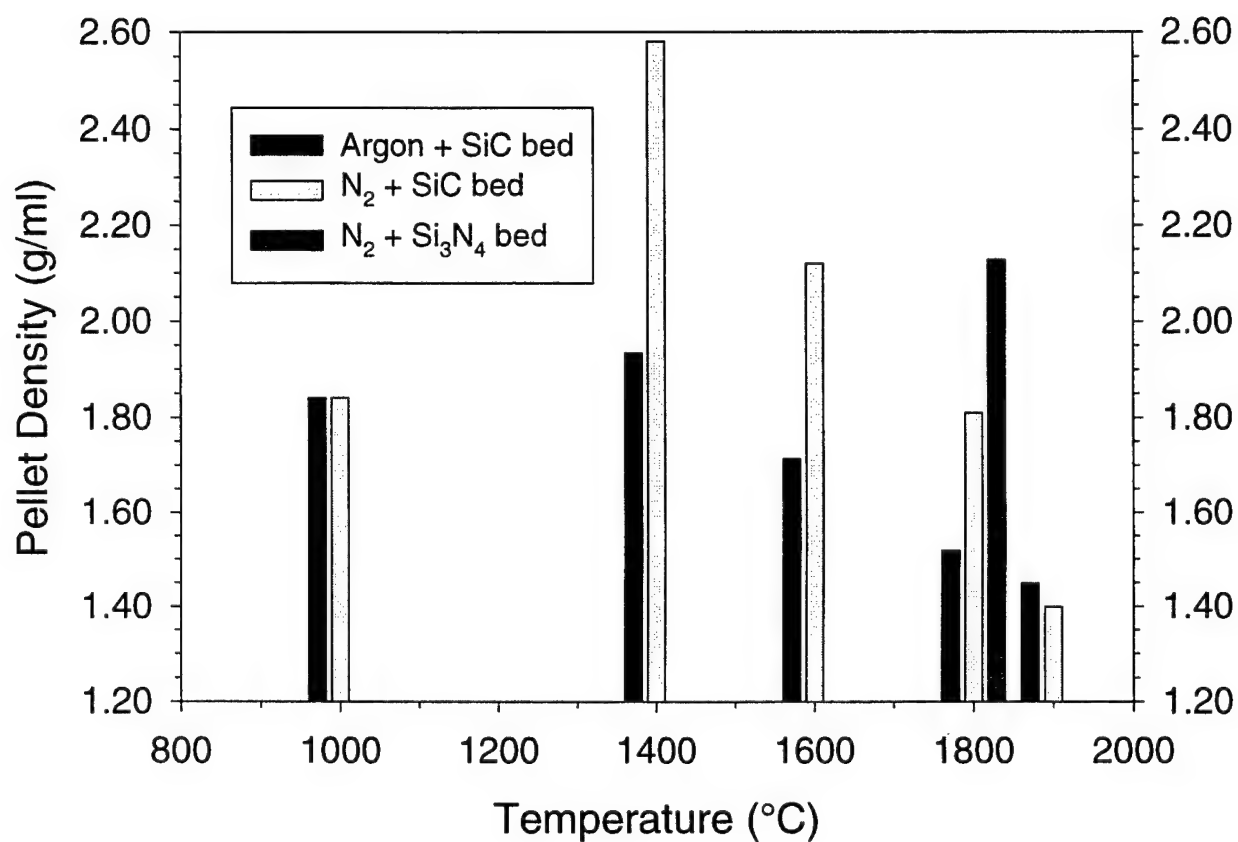




FIGURE 24

# AeroChem $\beta$ -SiC 2 hr firing at Temperature

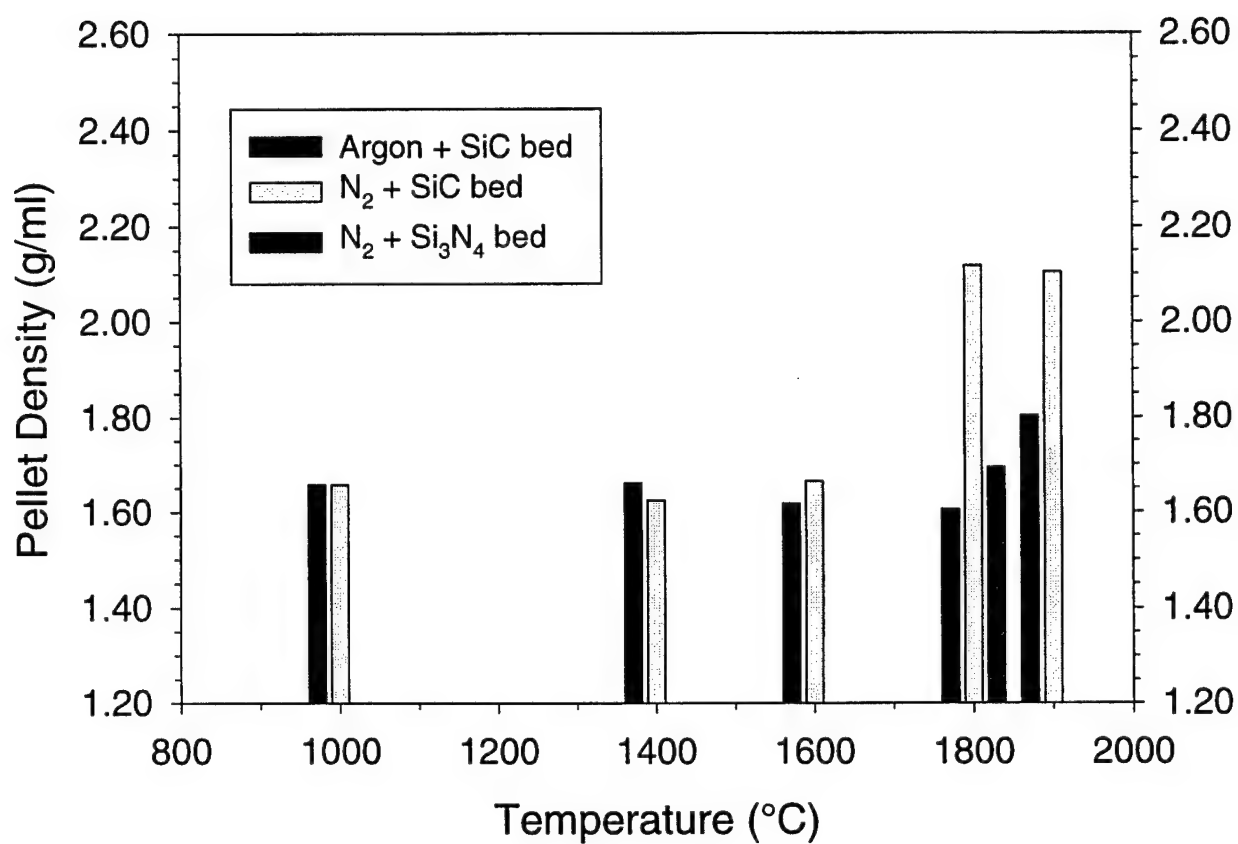


FIGURE 25

Washington Mills  $\alpha$ -SiC  
2 hr firing at Temperature

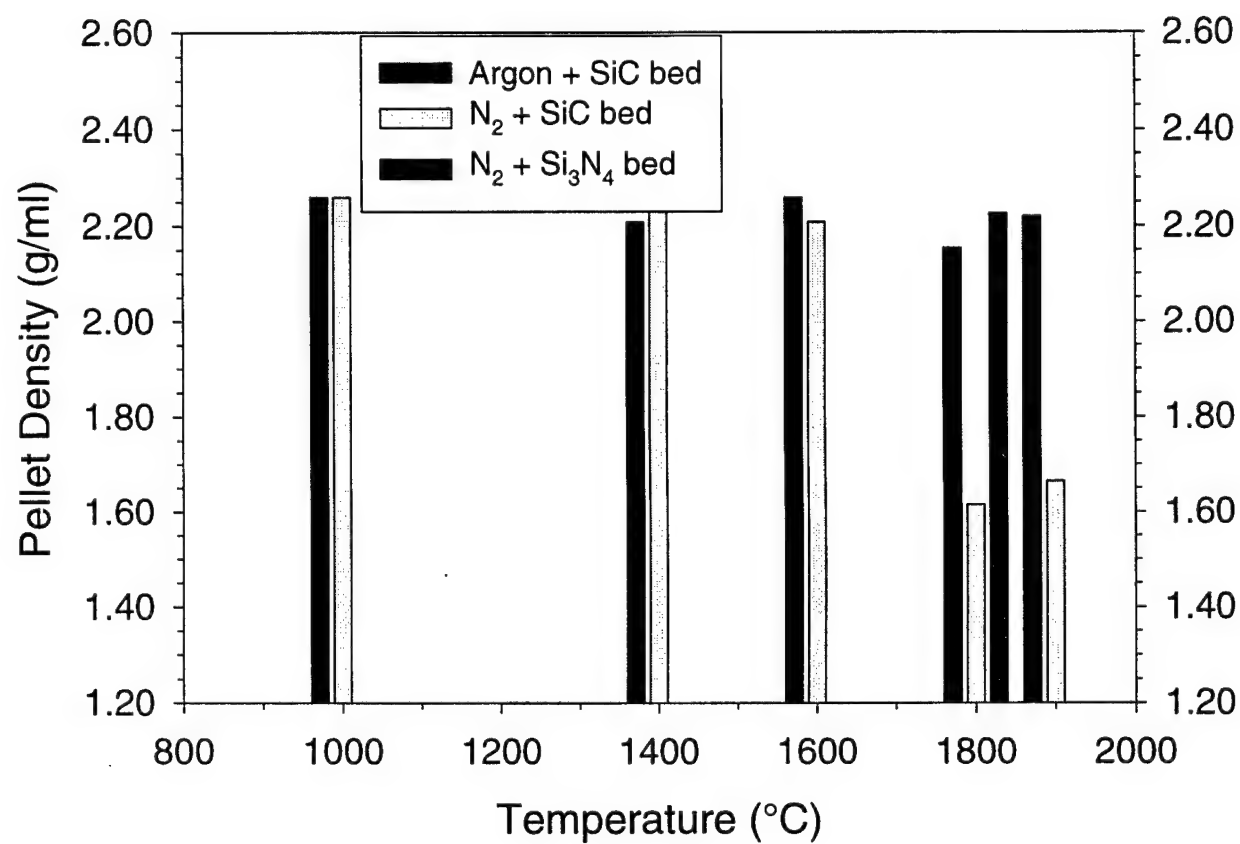


FIGURE 26

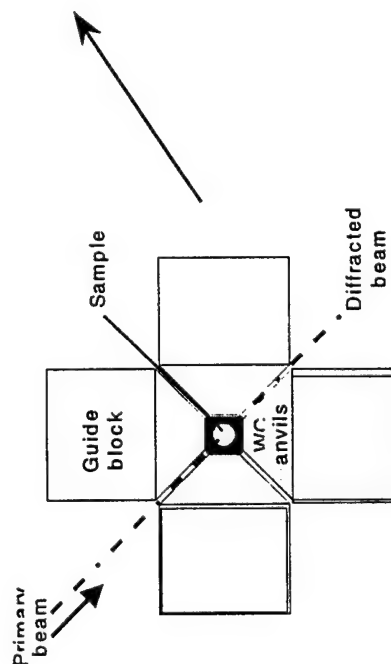
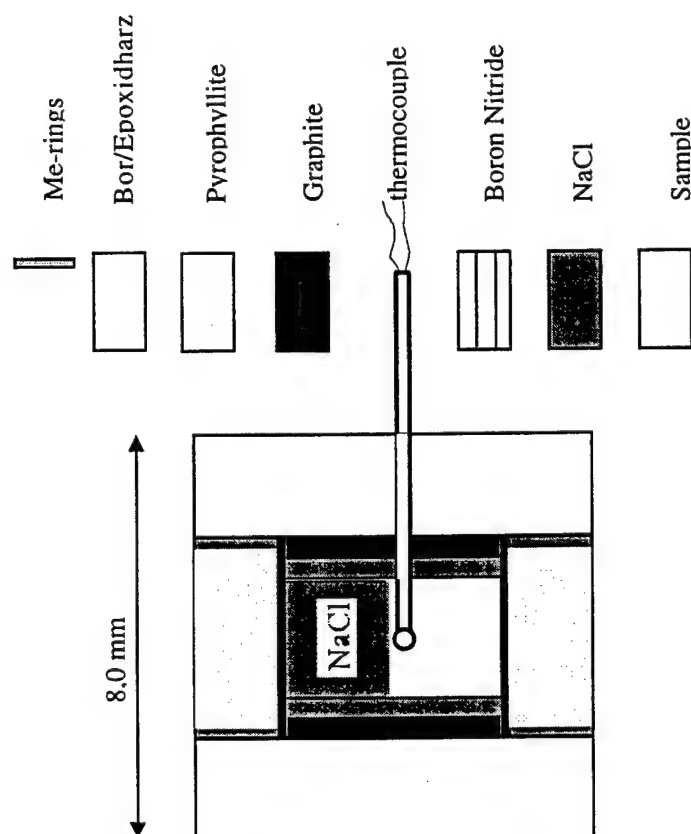
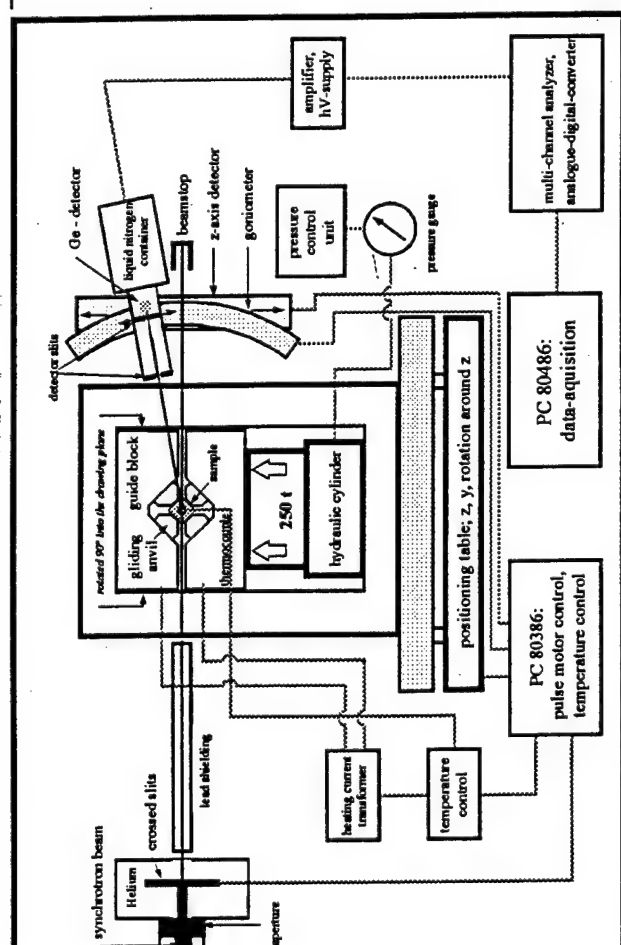
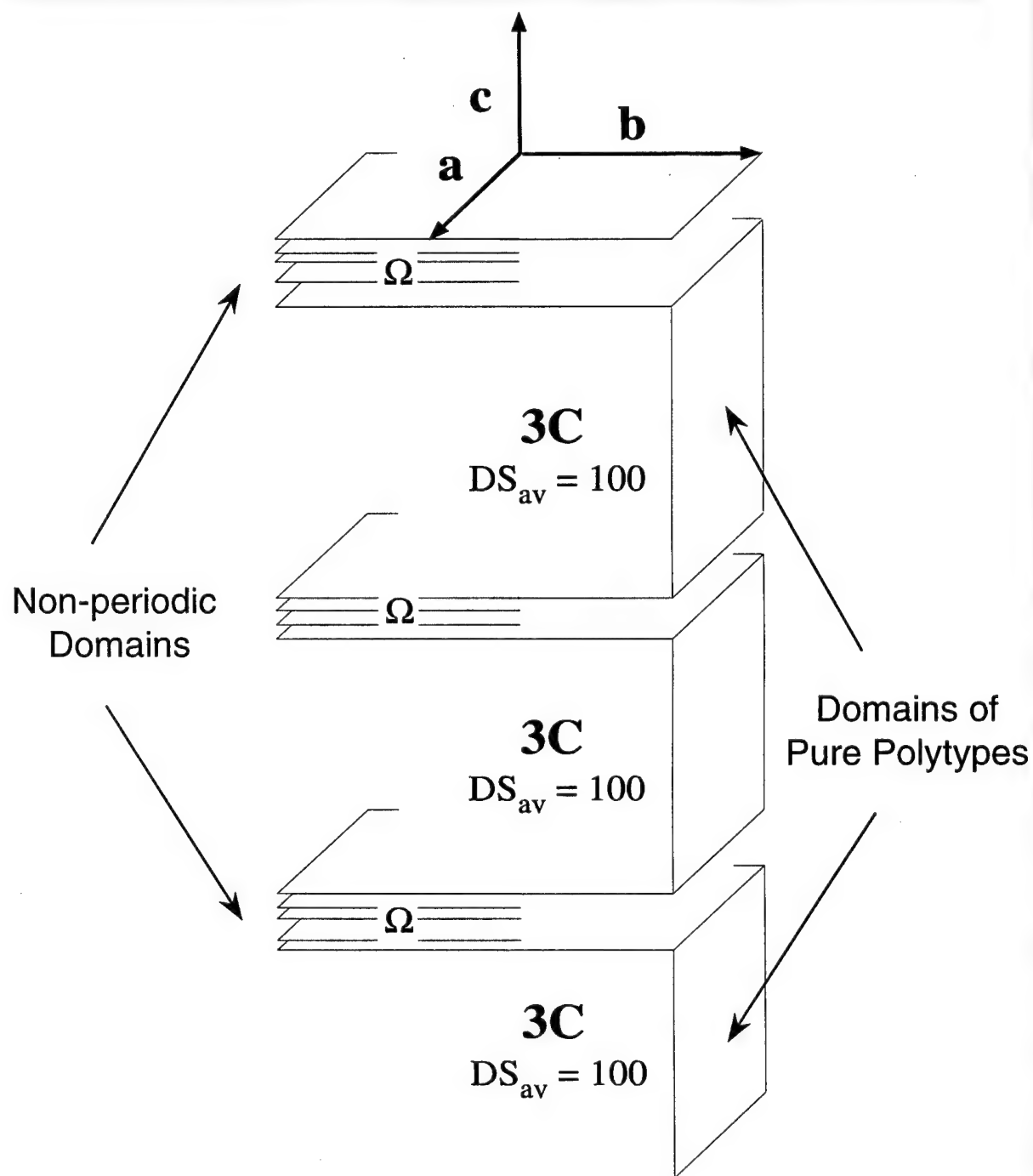


FIGURE 27

# A Model of a Disordered SiC Structure

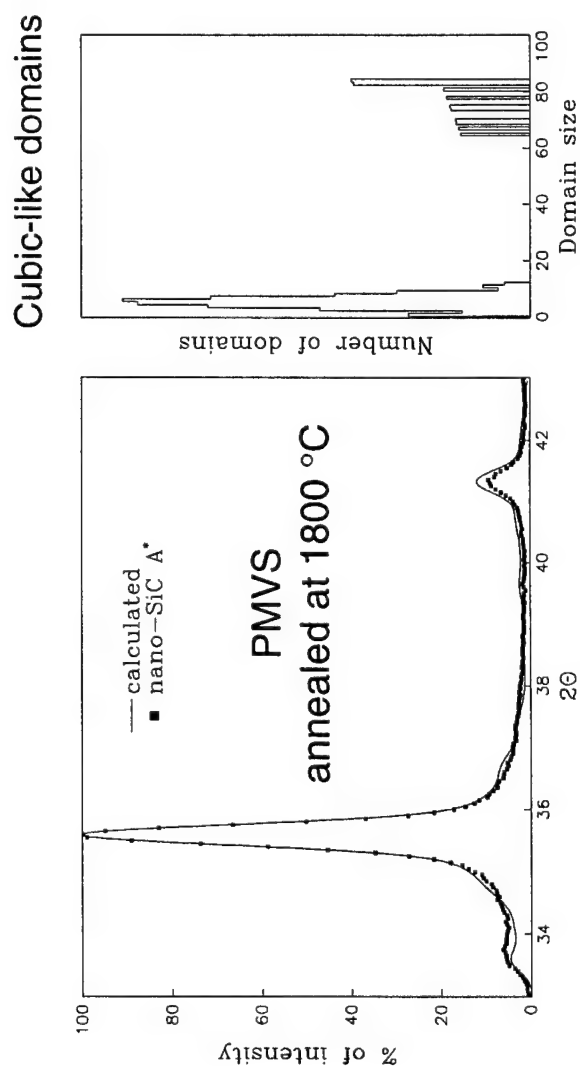


## DISTRIBUTION OF SiC POLYTYPES IN POLYMER-DERIVED SAMPLES

### DOMAIN DESCRIPTION

SAMPLE	3C	Cubic-like	2H-like	%Total Hex.
PMVS (C-Rich SiC)	35% ~50 layers	60% 3-4 layers	4% 2-3 unit cells	25%
PMVS/PHPS-B (xs Si/xs C = 0.25)	60% ~50 layers	34% ~9 layers	6%	16%
PMVS/PHPS-C (xs Si/xs C = 0.50)	78% ~50 layers	20% ~4 layers	1-2%	7-8%

SAMPLES WERE PROCESSED IN ARGON TO 1800 °C FOR 1 HR

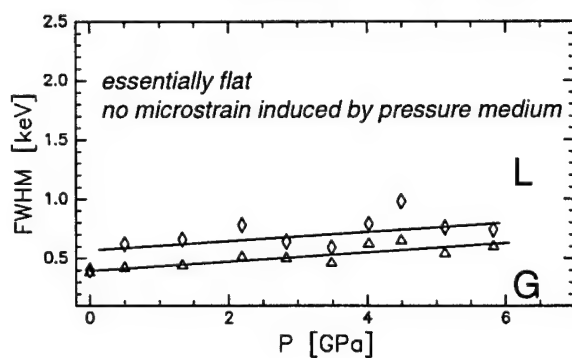


In contrast to  $\alpha$ - and  $\beta$ -SiC microcrystalline powders, nanocrystalline materials do not show changes of their polytype structure upon heating under pressure.

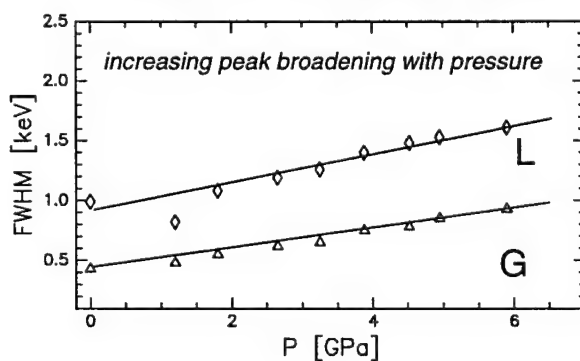
## PRESSURE-INDUCED MICROSTRAIN

PMVS/PHPS-C 1800 °C  
*measurements of the 3C (022) plane*

### HYDROSTATIC CONDITIONS

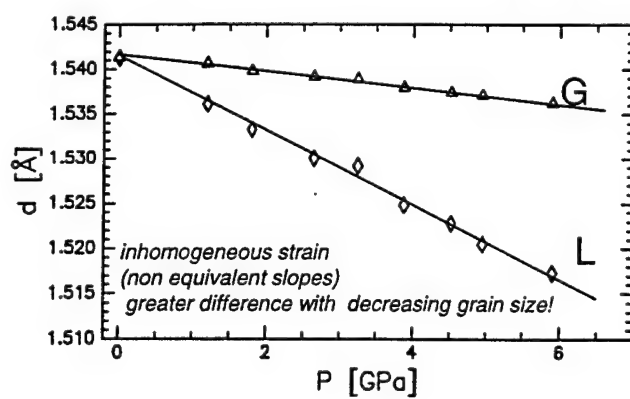


### ISOSTATIC CONDITIONS



PMVS/PHPS-C 1800 °C  
*measurements of the 3C (022) plane*

ISOSTATIC CONDITIONS

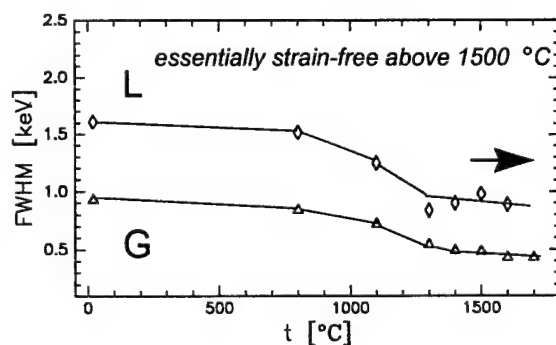




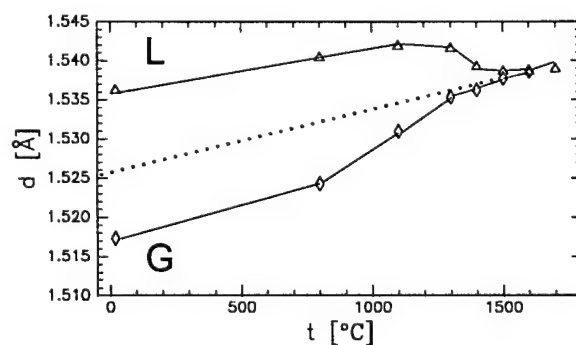
## RELAXATION OF MICROSTRAIN AT HIGH TEMPERATURE UNDER PRESSURE

PMVS/PHPS-C 1800 °C  
*measurements of the 3C (022) plane*

### ISOSTATIC CONDITIONS

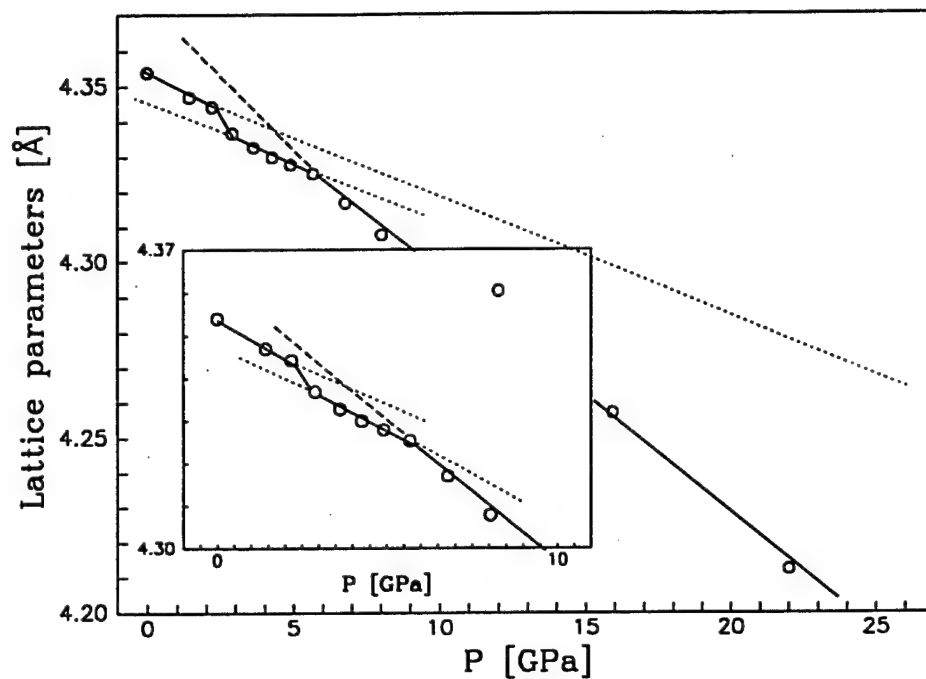


### ISOSTATIC CONDITIONS

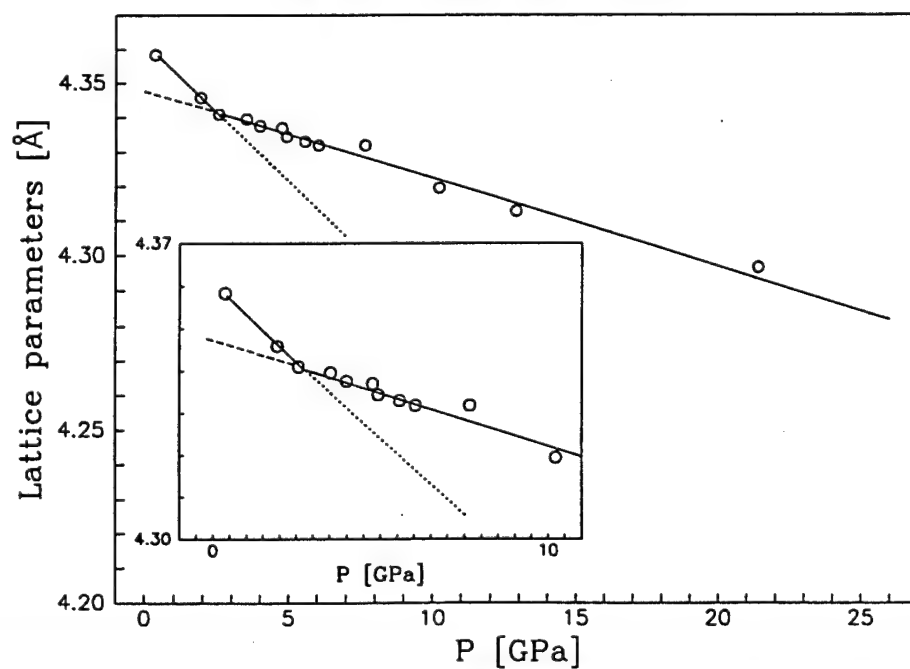


# COMPRESSIBILITY STUDIES USING DAC

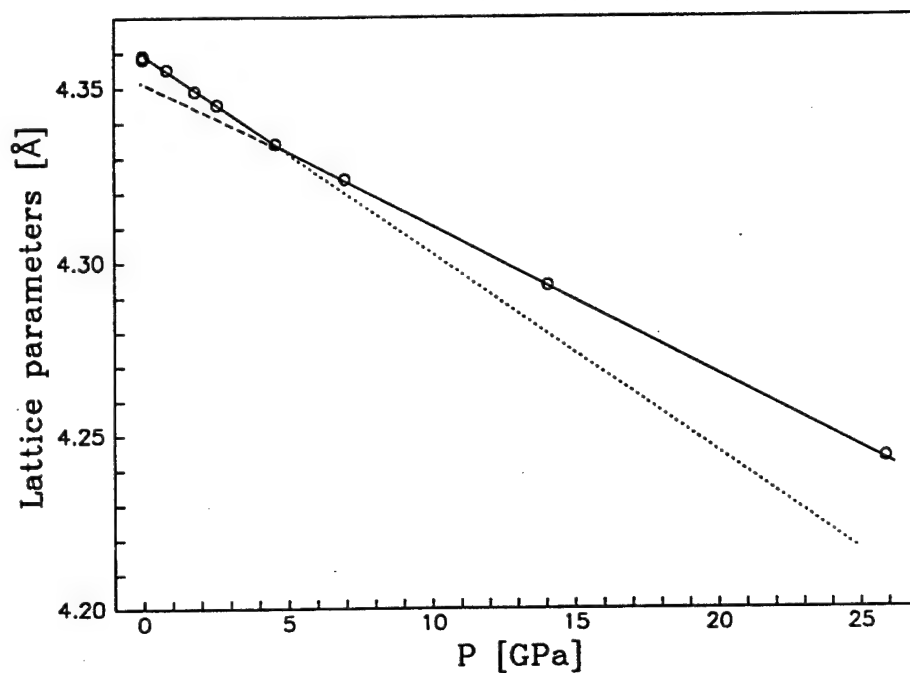
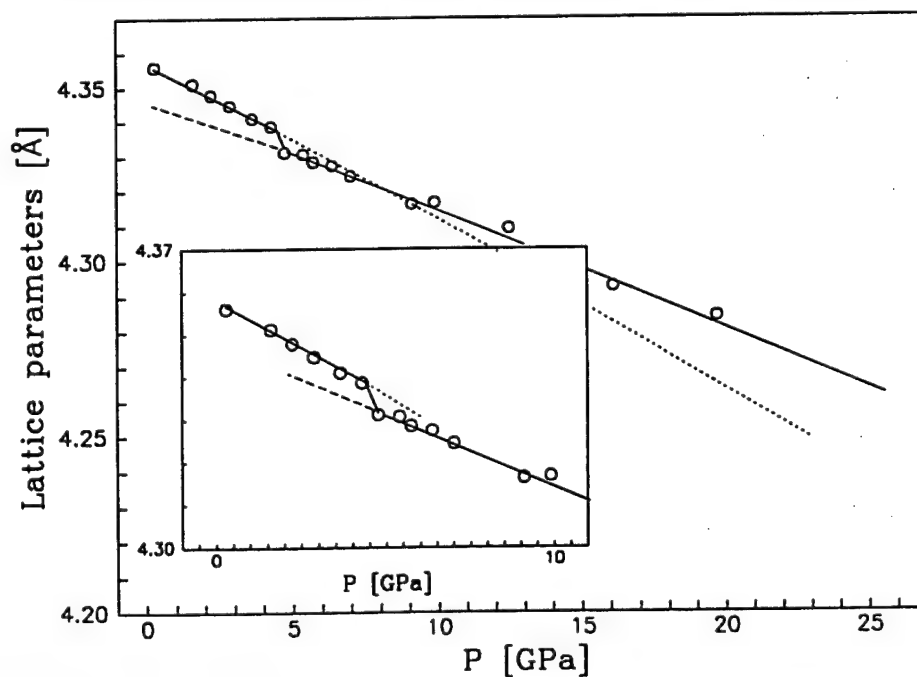
*PMVS A (xs C) 1600 °C*



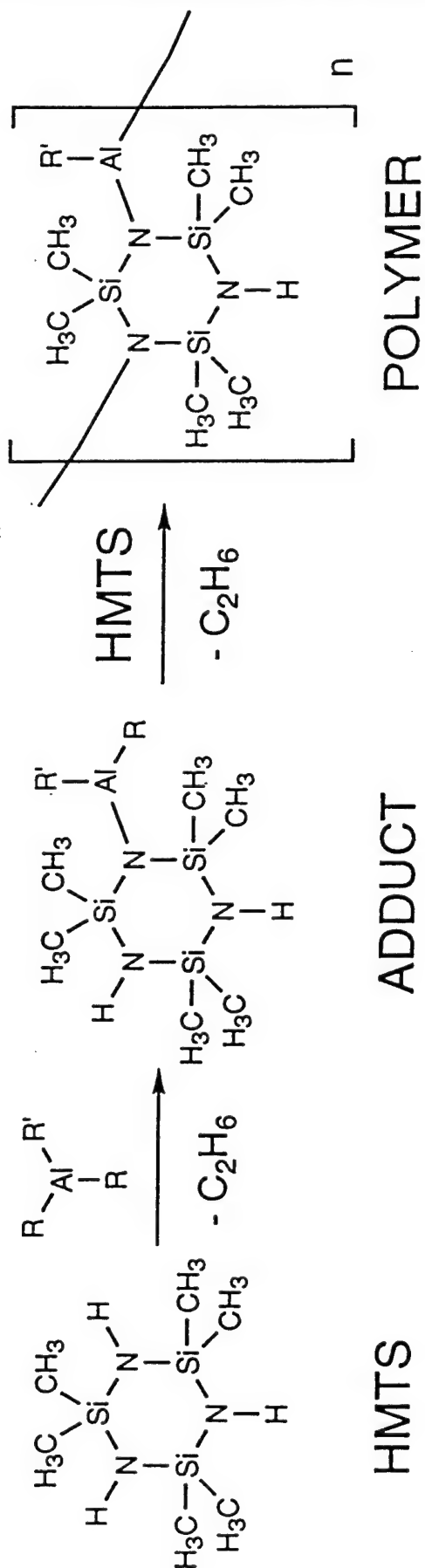
*PMVS A (xs C) 1800 °C*



## COMPRESSABILITY STUDIES USING DAC

*MICROCRYSTALLINE  $\beta$ -SiC**PMVS/PHPS-C ( $x_s$  Si/ $x_s$  C=0.5) 1800 °C*

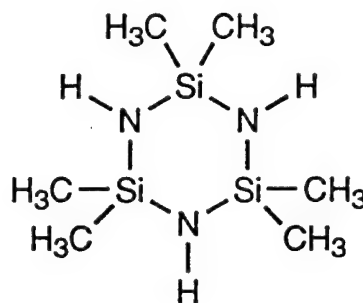
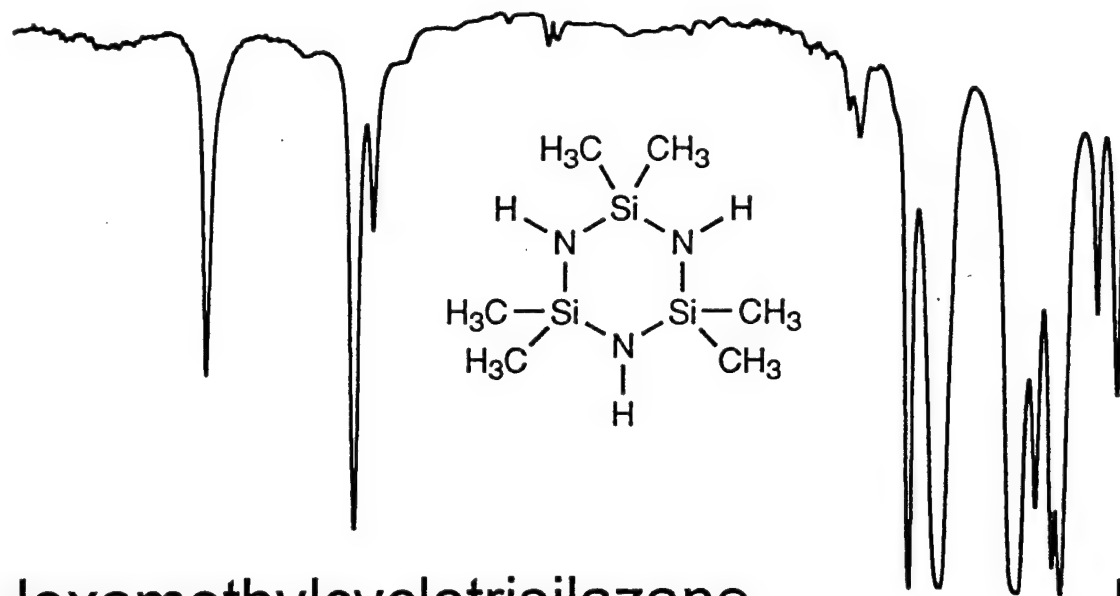
# SYNTHESIS OF SINGLE-SOURCE SiC/AlN PRECURSORS



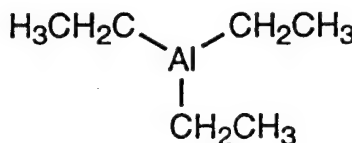
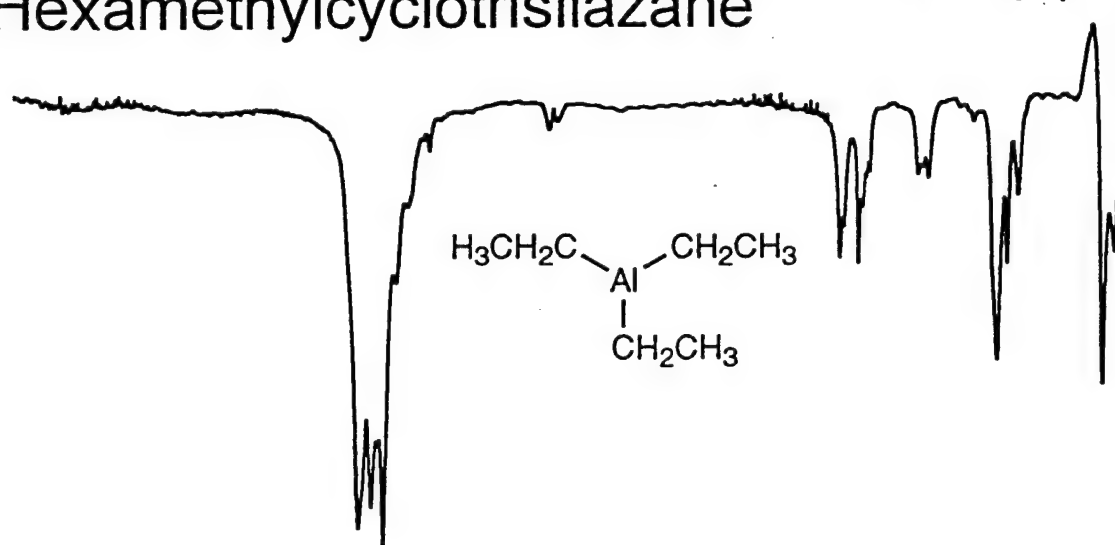
$\text{R} = \text{C}_2\text{H}_5, \quad \text{R}' = \text{C}_2\text{H}_5 \text{ (PAS)}$

$\text{PAS} = \text{POLY(ALUMINOSILAZANE)}$

4000 3500 3000 2500 2000 1500 1000 500



Hexamethylcyclotrisilazane



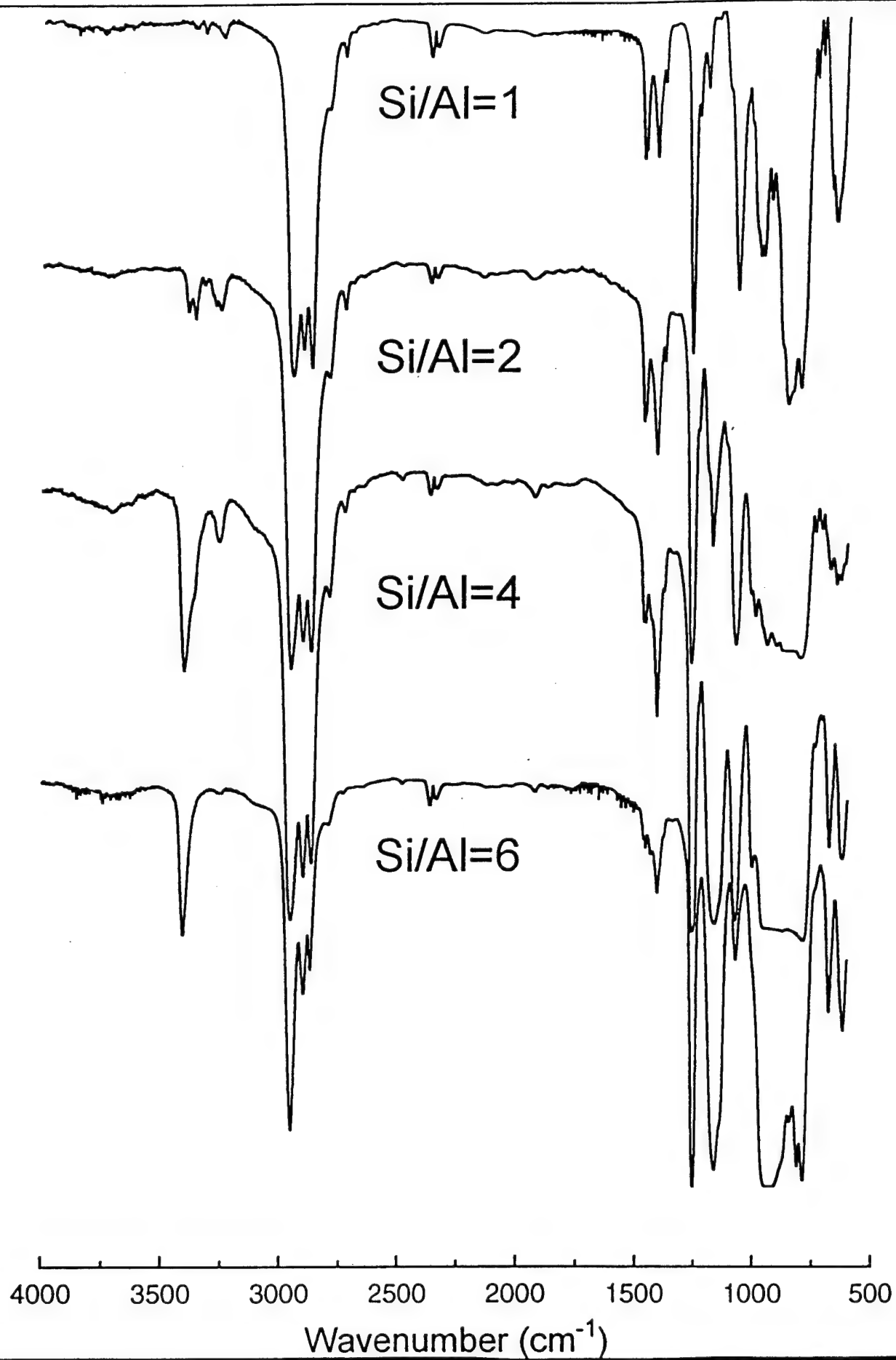
Triethylaluminum

4000 3500 3000 2500 2000 1500 1000 500

Wavenumber (cm⁻¹)



UNITED  
TECHNOLOGIES  
RESEARCH  
CENTER



# THERMAL ANALYSIS OF POLY(ALUMINOSILAZANE)

56.5 % CHAR YIELD  
@ 10 °C/MIN in N<sub>2</sub>

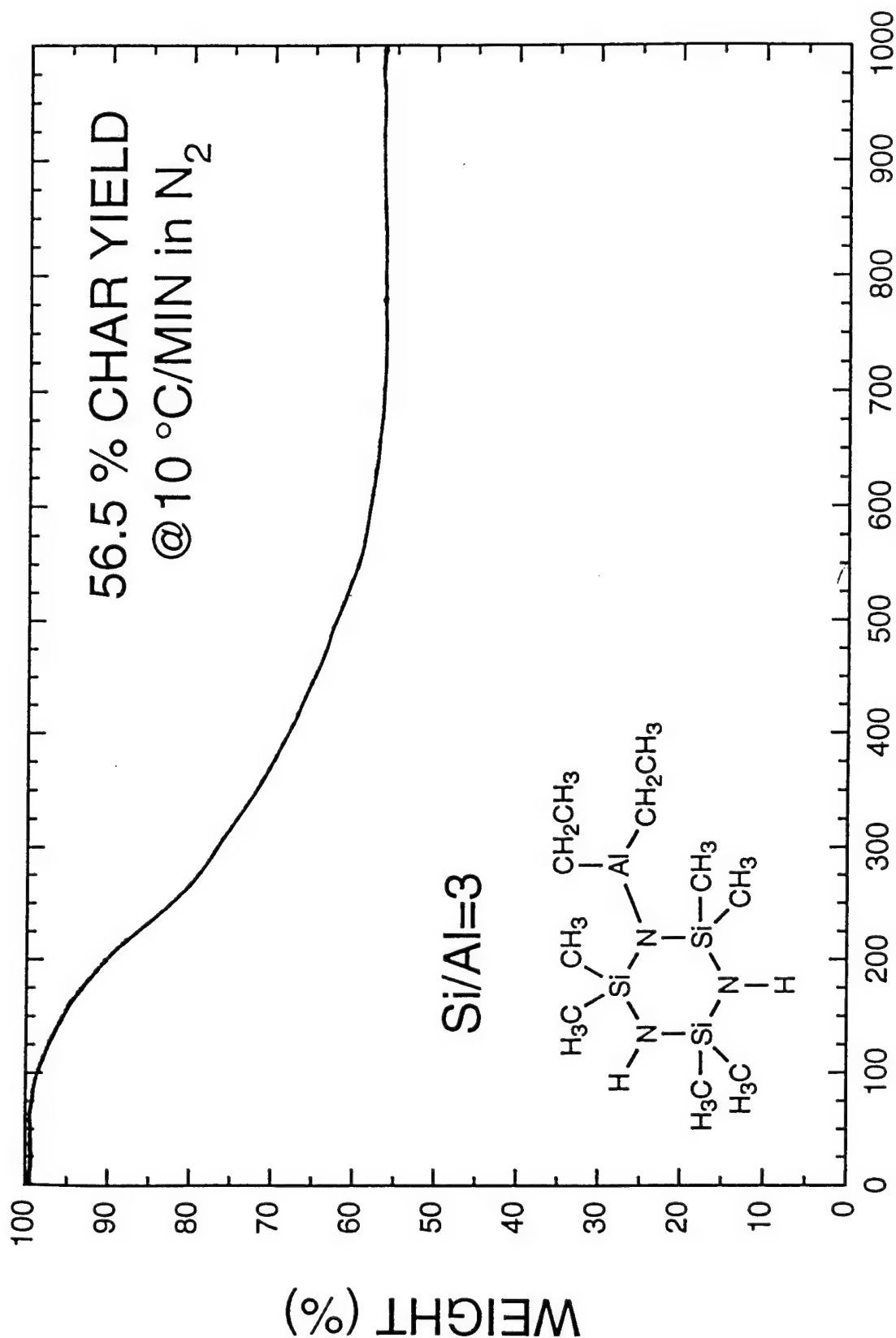
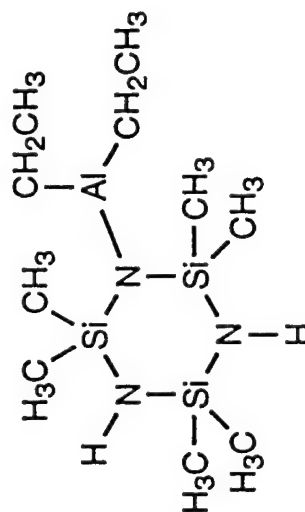
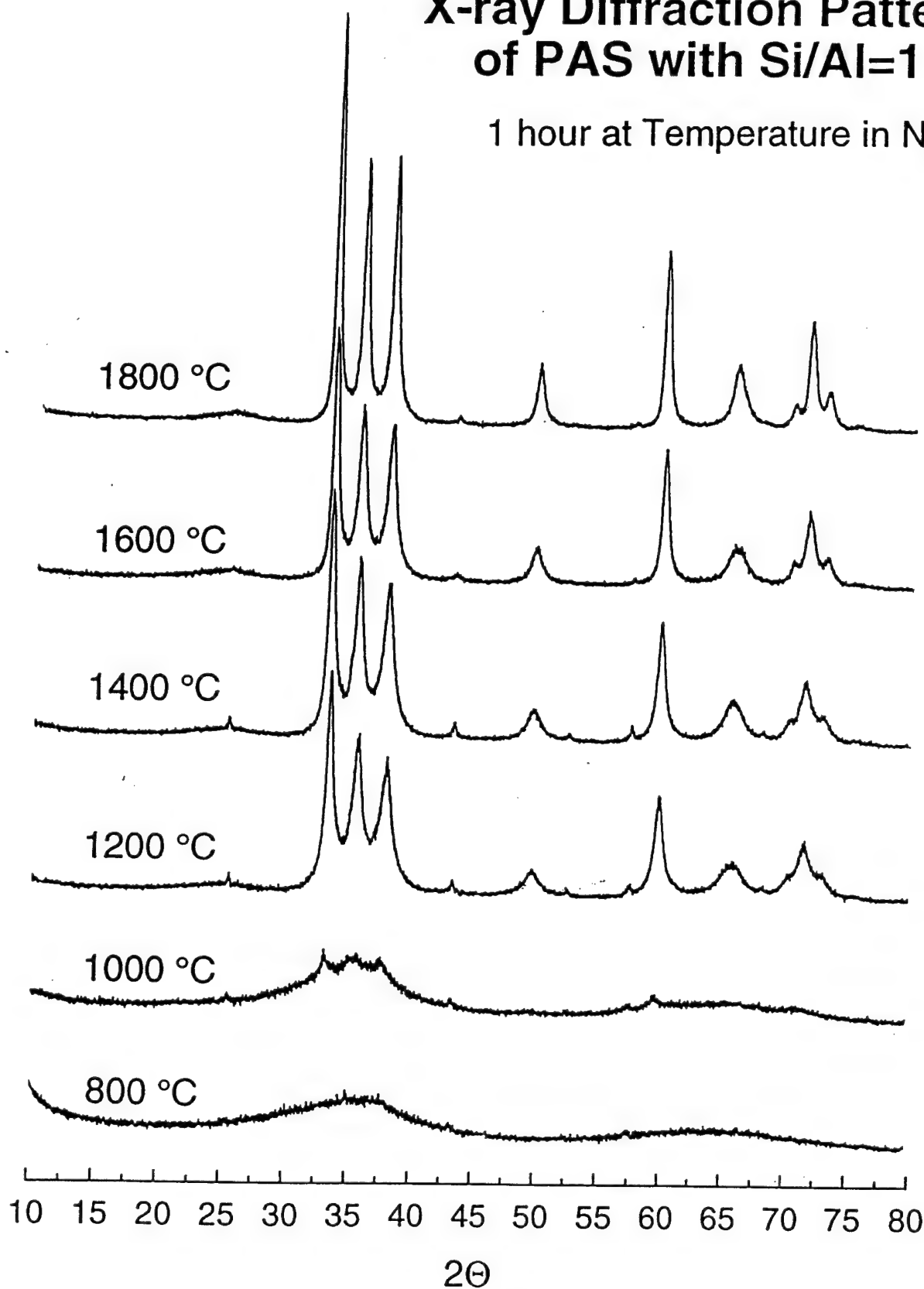
$$Si/Al=3$$


FIGURE 38



# X-ray Diffraction Patterns of PAS with Si/Al=1.0

1 hour at Temperature in N<sub>2</sub>



UNITED  
TECHNOLOGIES  
RESEARCH  
CENTER

TEM Micrographs of PAS with Si/Al = 1.0, Heated at 1800°C in N<sub>2</sub> for 1 hour

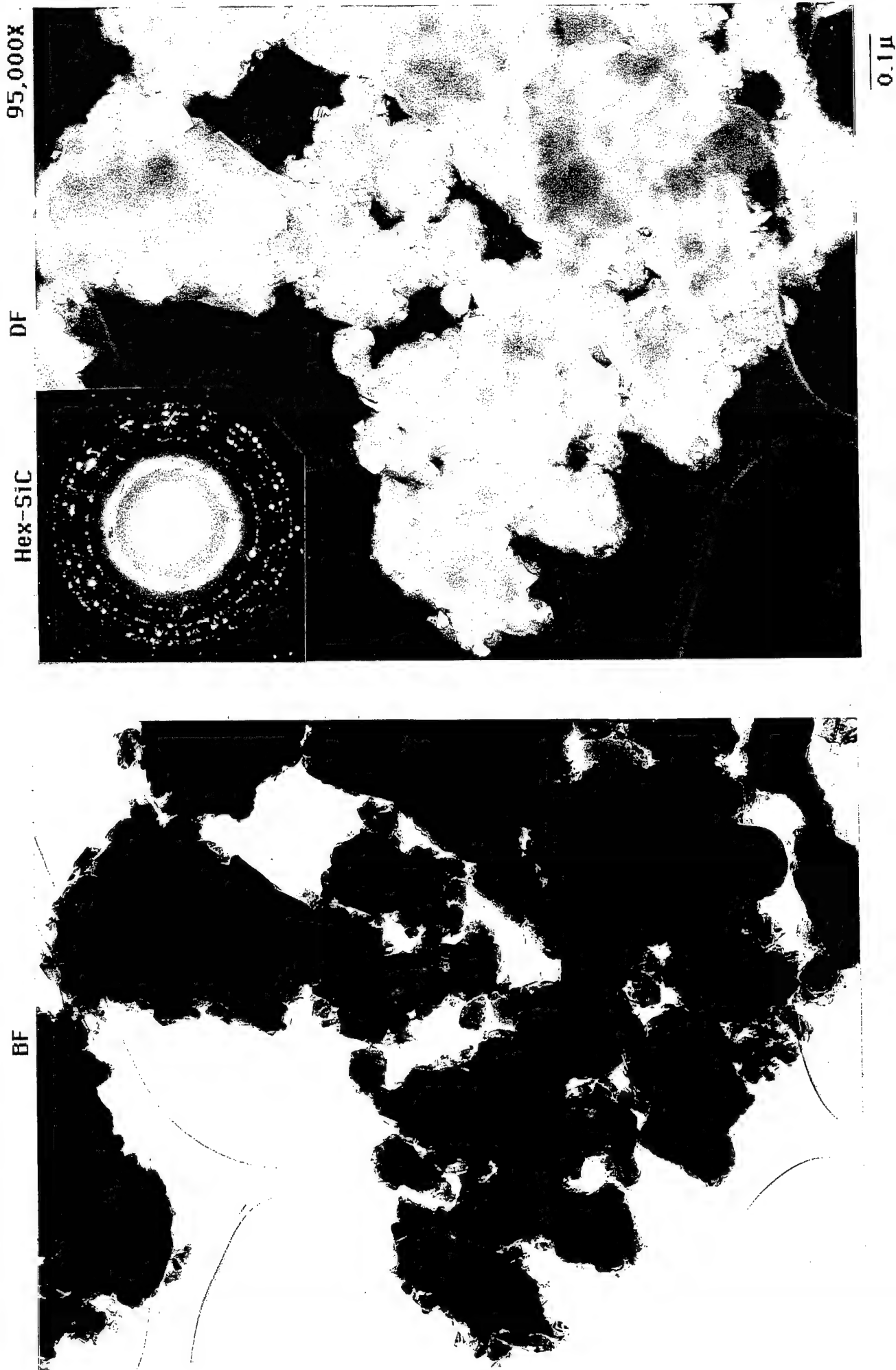
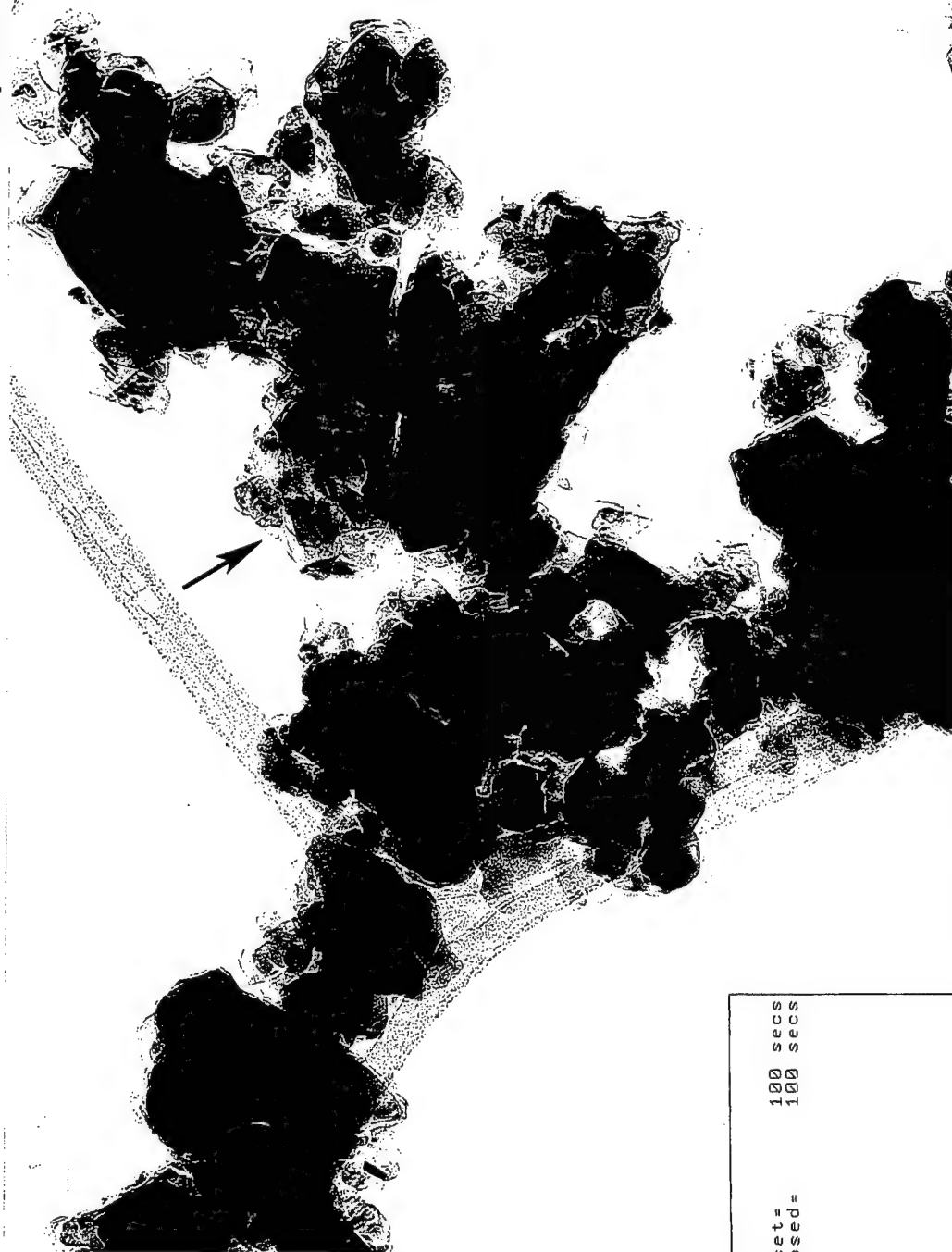


FIGURE 40

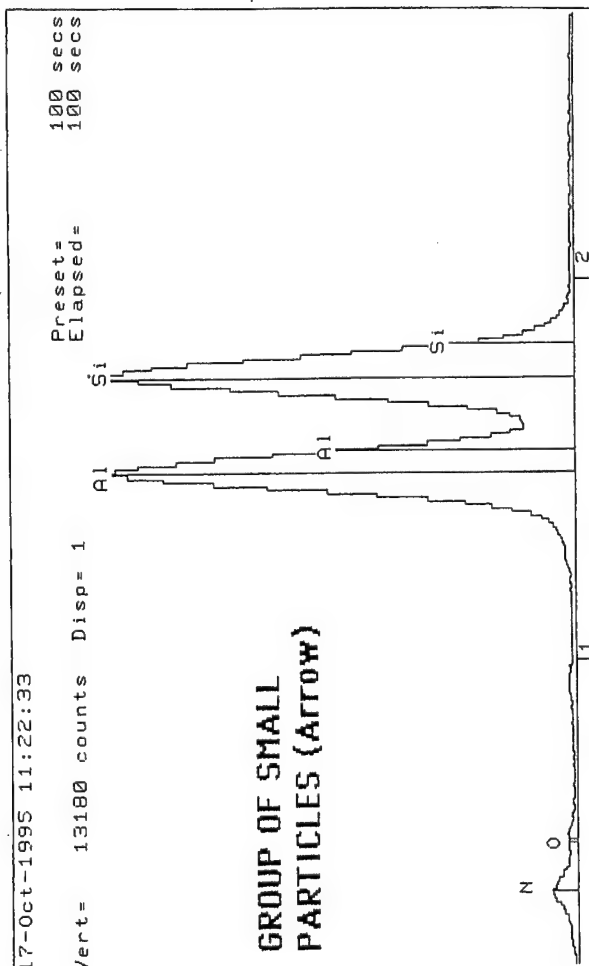
# TEM Micrograph of PAS with Si/Al = 1.0, Heated at 1800°C in N<sub>2</sub> for 1 hour

150,000X

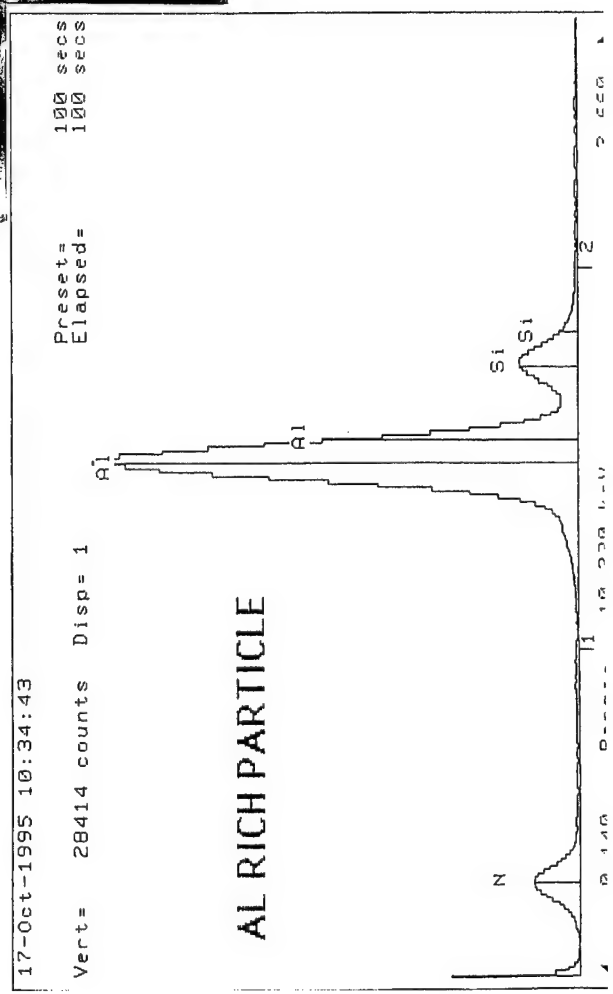


0.1μ

FIGURE 41



TEM Micrograph of PAS with Si/Al = 1.0, Heated at 1800°C in N<sub>2</sub> for 1 hour  
150,000X

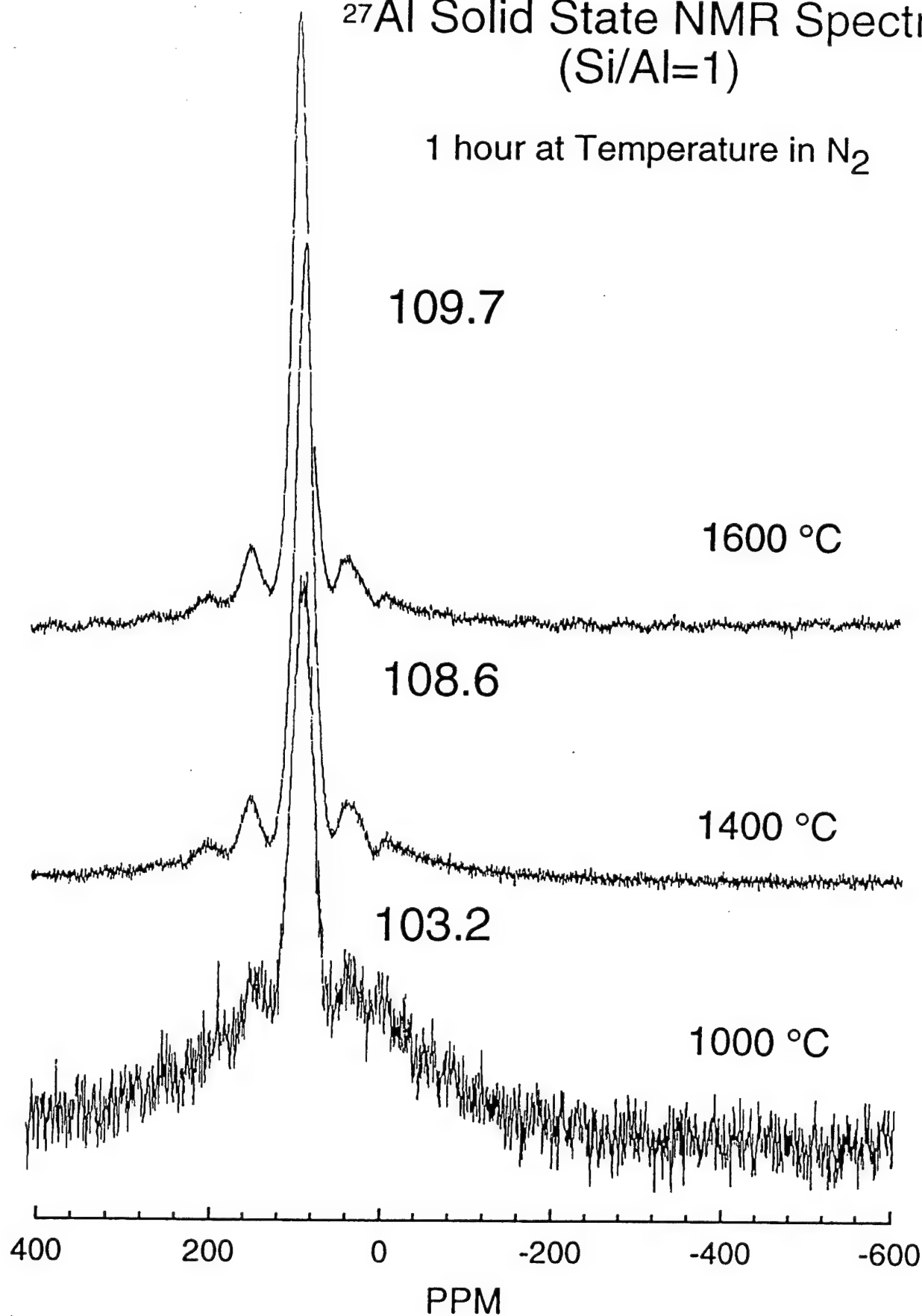


0.1μ

FIGURE 42

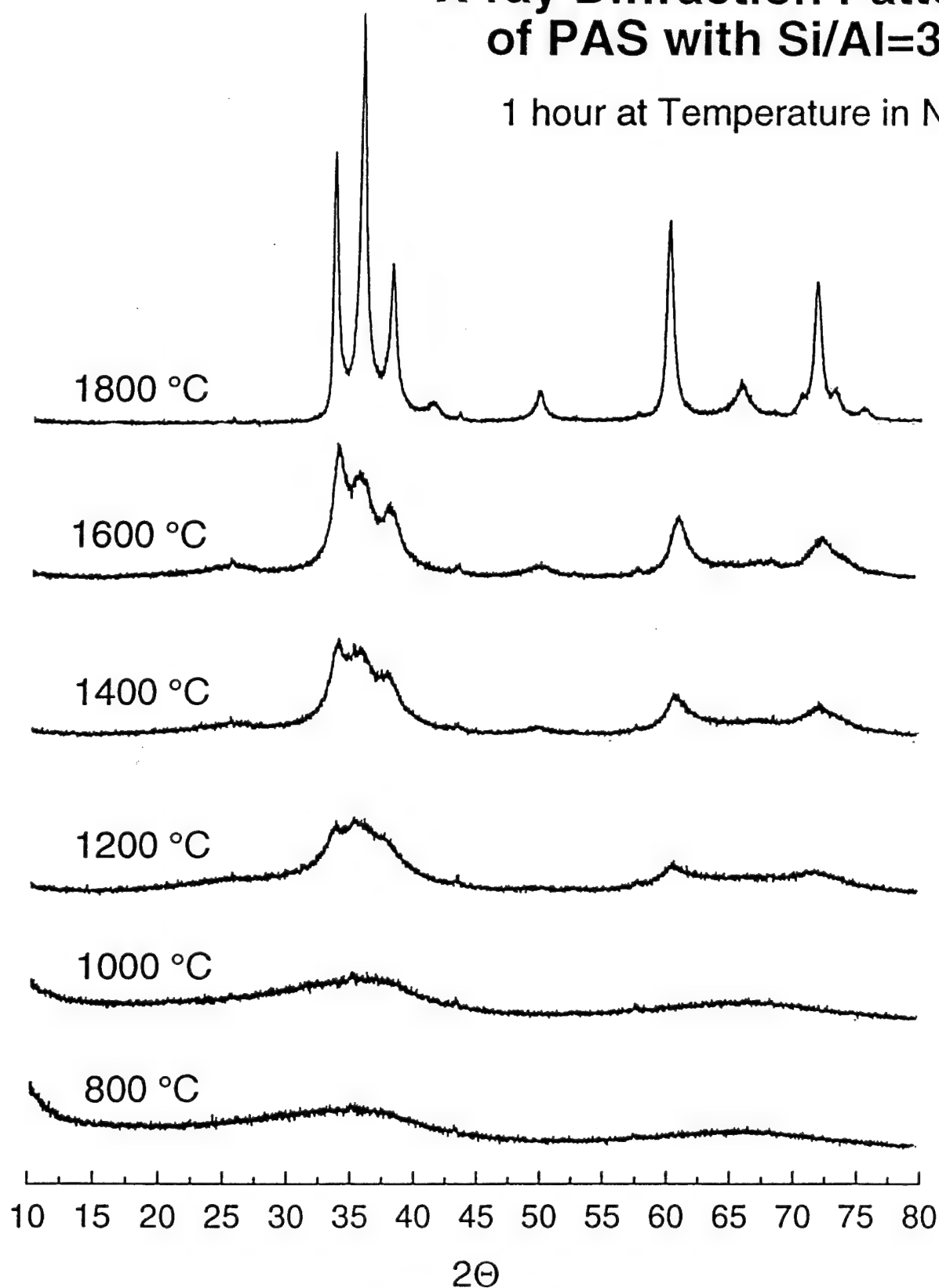
$^{27}\text{Al}$  Solid State NMR Spectra  
(Si/Al=1)

1 hour at Temperature in  $\text{N}_2$



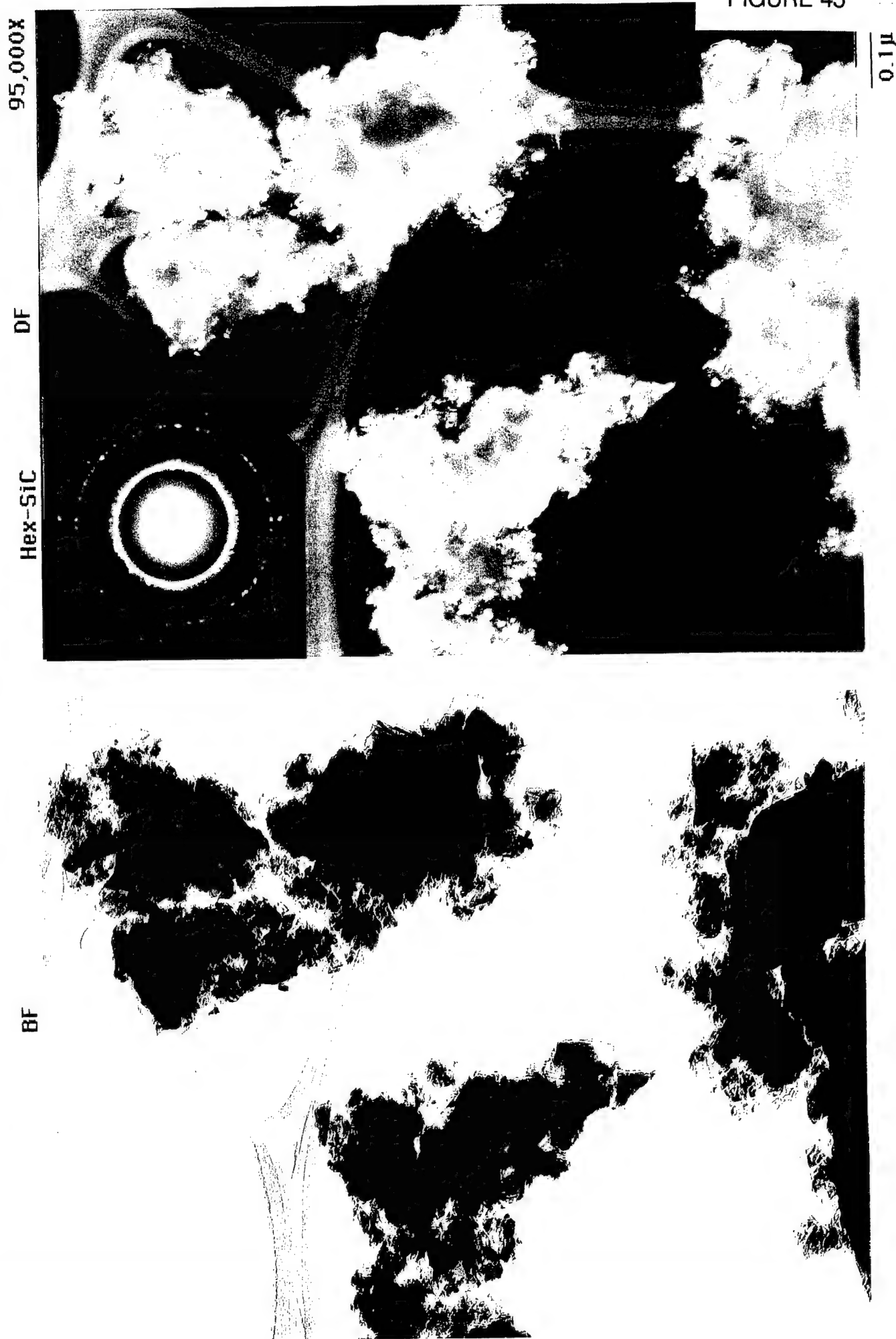
# X-ray Diffraction Patterns of PAS with Si/Al=3.0

1 hour at Temperature in N<sub>2</sub>



UNITED  
TECHNOLOGIES  
RESEARCH  
CENTER

TEM Micrographs of PAS with Si/Al = 3.0, Heated at 1800°C in N<sub>2</sub> for 1 hour





TEM Micrograph of PAS with Si/Al = 3.0, Heated at 1800°C in N<sub>2</sub> for 1 hour

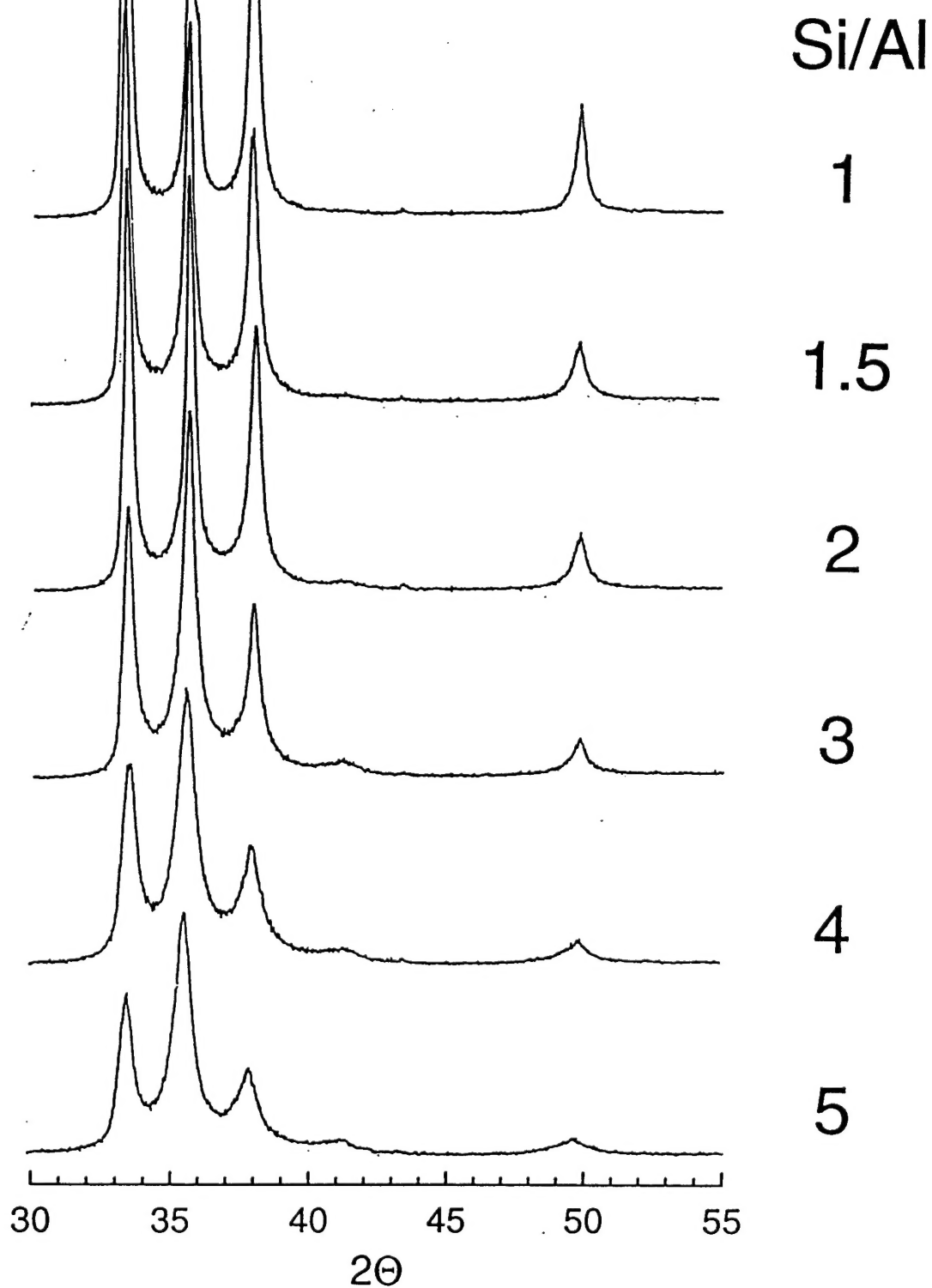
425,000X



0.05μ

# PAS X-ray Diffraction Patterns

1 hour at 1800 °C in N<sub>2</sub>



# XRD Patterns of PAS Heated to 1800 °C for 1 hour in N<sub>2</sub>

